Parkin is transcriptionally regulated by ATF4: evidence for an interconnection between mitochondrial stress and ER stress

Konstanze F. Winklhofer, Lena Bouman, Anita Schlierf, A. Kathrin Lutz, Jixiu Shan, Alexandra Deinlein, Jessica Kast, Zohreh Galehdar, Vincenza Palmisano, Nadja Patenge, et al.

Parkin is transcriptionally regulated by ATF4:

evidence for an interconnection between mitochondrial stress and ER stress

Lena Bouman[1], Anita Schlierf[1], A. Kathrin Lutz[1], Jixiu Shan[2], Alexandra Deinlein[1], Jessica Kast[1], Zohreh Galehdar[3], Vincenza Palmisano[1], Nadja Patenge[5], Daniela Berg[5], Thomas Gasser[5], Regina Augustin[6], Dietrich Trümbach[6], Isabella Irrcher[3], David S. Park[3,4], Wolfgang Wurst[6,7], Michael S. Kilberg[2], Jörg Tatzelt[1] and Konstanze F. Winklhofer[1*]

[1]Adolf Butenandt Institute, Neurobiochemistry, Ludwig Maximilians University, Schillerstr. 44, 80336 Munich, Germany; [2]Department of Biochemistry and Molecular Biology, Genetics Institute, Shands Cancer Center and Center for Nutritional Sciences, University of Florida College of Medicine, Gainesville, FL 32610, USA; [3]Cellular and Molecular Medicine, University of Ottawa, Ottawa, Canada; [4]Department of Cogno-Mechatronics Engineering, Pusan National University, South Korea; [5]Department of Neurodegeneration, Hertie Institute for Clinical Brain Research, University of Tübingen, and German Center for Neurodegenerative Diseases Hoppe-Seyler-Str. 3, 72076 Tübingen, Germany; [6]Helmholtz Centre Munich, German Research Centre for Environmental Health, Technical University Munich, Institute of Developmental Genetics, and German Center for Neurodegenerative Diseases, Ingolstaedter Landstr. 1, 85764 Munich/Neuherberg, Germany. [7]Max Planck Institute of Psychiatry, Kraepelinstr. 2, 80804 Munich, Germany.

*To whom correspondence should be addressed:

Konstanze F. Winklhofer, Schillerstr. 44, D-80336 Munich, telephone: +49 89 2180 75483, fax: +49 89 2180 75415, E-mail: Konstanze.Winklhofer@med.uni-muenchen.de

Running title: Parkin, ER stress and mitochondria

Key words: ATF4/ c-Jun/ER stress/JNK/parkin/Parkinson's disease/UPR

Abstract

Loss of parkin function is responsible for the majority of autosomal recessive parkinsonism. Here we show that parkin is not only a stress-protective, but also a stress-inducible protein. Both mitochondrial and endoplasmic reticulum (ER) stress induce an increase in parkin-specific mRNA and protein levels. The stress-induced up-regulation of parkin is mediated by ATF4, a transcription factor of the unfolded protein response (UPR) that binds to a specific CREB/ATF site within the parkin promoter. Interestingly, c-Jun can bind to the same site, but acts as a transcriptional repressor of parkin gene expression. We also present evidence that mitochondrial damage can induce ER stress, leading to the activation of the UPR and thereby to an up-regulation of parkin expression. Vice versa, ER stress results in mitochondrial damage, which can be prevented by parkin. Notably, the activity of parkin to protect cells from stress-induced cell death is independent of the proteasome, indicating that proteasomal degradation of parkin substrates cannot explain the cyto-protective activity of parkin. Our study supports the notion that parkin plays a role in the interorganellar crosstalk between the ER and mitochondria to promote cell survival under stress, suggesting that both ER and mitochondrial stress can contribute to the pathogenesis of Parkinson's disease.

Introduction

Mitochondrial dysfunction has long been implicated in the pathogenesis of Parkinson's disease (PD). Mitochondrial toxins targeting complex I of the electron transport chain can induce acute parkinsonism in humans and are being used to model PD in animals. In line with a crucial role of mitochondrial function, complex I activities were reported to be reduced in the substantia nigra and less consistently, also in peripheral tissues from PD patients. More recently, several PD-associated genes have been shown to influence mitochondrial function, morphology, dynamics and turnover (rev. in (1-3). In addition to mitochondrial dysfunction several lines of evidence indicate that ER stress may contribute to the pathogenesis of PD (rev. in (4, 5). First, toxins such as MPTP, 6-OHDA or rotenone, used to induce parkinsonism in animal models, have been shown to cause ER stress (6-13). Second, ER stress accounts for at least some aspects of α-synuclein toxicity. α-Synuclein has been shown to block ER to Golgi vesicular trafficking in different model systems (14), and overexpression of α-synuclein can induce ER stress (14-16). Finally, ER stress has been documented in dopaminergic neurons of the parkinsonian substantia nigra, exemplified by increased levels of phospho-PERK, phospho-eIF2α and caspase-4 (17, 18). The link between PD and ER dysfunction was recently reinforced by the observation that the E3 ubiquitin ligase parkin can protect cells from ER stress-induced cell death induced by the overexpression of Pael-R, a putative parkin substrate which is prone to misfolding within the secretory pathway (19-22). Mutations in the parkin gene were identified as a cause of autosomal recessive PD with juvenile onset in Japanese families (23). Since then, more than one hundred different mutations have been described in patients of diverse ethnic backgrounds, accounting for the majority of autosomal recessive parkinsonism (24).

ER stress originates from the accumulation of un- or misfolded secretory proteins, perturbations in calcium homeostasis or redox status, alterations in glycosylation, or energy

deprivation. The ER has evolved sophisticated stress response signaling pathways collectively called the unfolded protein response (UPR), destined to increase the ER folding capacity, to reduce the ER folding load and to restore ER homeostasis (rev. in (25-27). Conversely, when ER stress conditions are severe or persistent, apoptotic cell death is induced (rev. in (28-31). The sensing and transduction of ER stress is orchestrated by three ER transmembrane proteins, PERK, ATF6 and IRE1. PERK (double-stranded RNA-activated protein kinase-like ER kinase) induces an immediate and transient attenuation of protein biosynthesis via phosphorylation of eIF2α (eukaryotic translation initiation factor 2α). Phosphorylated eIF2α inhibits general translation initiation, but allows selective translation of some mRNAs, such as ATF4 (activating transcription factor 4). Activation of ATF6 (activating transcription factor 6) involves regulated intramembrane proteolysis in the Golgi complex, resulting in an active transcription factor for UPR target genes. IRE1 (inositol requiring kinase 1) is a bifunctional protein which is trans-autophosphorylated upon ER stress to activate its RNase activity. Cleavage of XBP1 (X-box binding protein 1) mRNA by activated IRE1 leads to the generation of a transcription factor responsible for the expression of various UPR target genes.

Recent research revealed that the ER physically and functionally interacts with mitochondria to influence key aspects of cellular physiology and viability (rev. in (32, 33). Interactions between these organelles allow the exchange of metabolites and are implicated in the regulation of calcium signaling and cell death pathways. Our study shows that parkin expression is increased upon ER stress and mitochondrial stress via the PERK/ATF4 branch of the UPR. Increased expression of parkin prevents ER stress-induced mitochondrial damage and cell death, providing evidence for a functional link between parkin, ER stress and mitochondrial integrity.

Results

Mitochondrial membrane dissipation induced by CCCP causes ER stress and leads to a transcriptional up-regulation of parkin

The protonophore CCCP (carbonyl cyanide m-chlorophenyl hydrazone) is being used to induce mitochondrial damage in various model systems. CCCP renders the mitochondrial inner membrane permeable for protons and causes dissipation of the proton gradient across the inner mitochondrial membrane. We recently observed that the complex I inhibitor rotenone induces an up-regulation of parkin-specific mRNA and protein levels (34). CCCP has recently been shown to cause the translocation of parkin to damaged mitochondria, which are then removed by autophagy (35-39). We therefore addressed the question of whether CCCP might also have an impact on the transcriptional regulation of parkin. Human neuroblastoma-derived SH-SY5Y cells were incubated with CCCP (10 μM) for the indicated time and parkin-specific mRNA levels were analyzed by quantitative RT-PCR. Parkin mRNA levels were significantly increased after CCCP treatment (Fig. 1 A). This phenomenon was also observed in CCCP-treated primary mouse cortical neurons (Fig. 1 B). To get insight into the mechanism underlying the regulation of parkin gene expression, we screened the parkin promoter for possible binding sites of stress-regulated transcription factors by using TFSEARCH (Searching transcription Factor Binding Sites, http://www.rwcpor.jp/papia (40). We discovered a putative CREB/ATF site in the parkin promoter that is located at –169 to –161 bp relative to the transcriptional start site (TSS). A further in-depth analysis identified this site as a possible binding sequence for ATF4 (Fig. 1 C and 3 A). The CREB/ATF site within the parkin promoter is conserved among species (*Homo sapiens*, *Mus musculus*, *Bos taurus* and *Equus caballus*, Fig. 1 C), supporting the notion that this site might be functionally relevant (41). An additional binding site is located downstream of the transcriptional start site

within the first intron of human, bovine and rodent parkin, which in addition to the other ATF4-binding site may play a role in the regulation of parkin expression (Fig. 1 C).

ATF4 is a transcription factor which is activated in response to ER stress. Some toxins used to model PD, such as MPTP and rotenone, have been associated with ER stress, therefore we analyzed whether mitochondrial membrane dissipation induced by CCCP can cause ER stress. Transcriptional/translational regulation of genes in response to ER stress is mainly mediated by the UPR, a stress response program that collectively re-establishes cellular homeostasis via the combinatorial action of specific transcription factors, which bind to ER stress-responsive elements in the regulatory regions of UPR target genes (rev. in (25, 27). To test whether CCCP induces ER stress, we cloned a luciferase reporter construct containing the ER stress-responsive element ERSE-II (ERSE-II-luc, Supplemental Fig. 5). Treatment of cells transiently expressing the luciferase reporter construct with the N-glycosylation inhibitor tunicamycin induced an increase in luciferase expression, demonstrating the functionality of this ER stress reporter construct (Fig. 1 D). Moreover, CCCP was also able to significantly increase luciferase expression from the ER stress reporter construct (Fig. 1 D). In addition, we quantified the mRNA of the ER chaperone BiP, which is a major target of the UPR. In line with the data from the ER stress luciferase reporter assay, CCCP treatment caused an up-regulation of BiP mRNA expression (Fig. 1 E), indicating that the mitochondrial toxin CCCP can indeed induce ER stress.

Parkin gene expression is up-regulated in response to ER stress

In a next step we tested whether gene expression of parkin is influenced by ER stress. SH-SY5Y cells were incubated with either the ER Ca^{2+}-ATPase inhibitor thapsigargin (TG) or the N-glycosylation inhibitor tunicamycin (TM). Parkin-specific mRNA levels were analyzed by quantitative RT-PCR. Both ER stressors significantly increased the level of parkin-specific mRNA with a maximum at 12 hours after drug treatment (Fig. 2 A, B).

Another classical inducer of ER stress is amino acid starvation (42). We therefore made use of L-histidinol, a histidine analogue which inhibits activation of histidine by histidyl-tRNA synthetase. Also in this ER stress paradigm, treating cells with L-histidinol for 15 hours led to an increase in parkin mRNA levels (Fig. 2 C). Employing mouse embryonic fibroblasts from PINK1 knockout mice, we observed that the up-regulation of parkin upon ER stress in not dependent on PINK1 expression (data not shown). Notably, the up-regulation of parkin in response to ER stress induced by thapsigargin, tunicamycin or L-histidinol was also observed on the protein level (Fig. 2 D, E, F) and was not restricted to SH-SY5Y cells since a significant up-regulation of parkin in response to thapsigargin or tunicamycin treatment was also observed in HEK293T cells, mouse embryonic fibroblasts, and primary neuronal cultures prepared from mouse cortex (Fig. 2 G, H, I).

Parkin is a target of the unfolded protein response (UPR) via the PERK/ATF4 pathway

To test whether the putative ATF4-binding site we discovered within the parkin promoter (–169 to –161 bp relative to TSS) can indeed mediate up-regulation of parkin in response to ER stress, we created a luciferase reporter construct using the pGL3-luc promoter vector containing the putative ATF4-binding site (in triplicate) in front of a sequence coding for luciferase (park-luc, Fig. 3 A). As a positive control, we cloned the confirmed ATF4-binding site of the insulin growth factor binding protein 1 (IGFBP1) promoter (43) analogously to the park-luc construct. This control construct was termed ATF4RE (**ATF4**-**r**esponsive **e**lement)-luc (Fig. 3 A). As a negative control, we cloned a mutant park-luc construct, harboring two point mutations in the putative ATF4-binding motif (mut. park-luc, Fig. 3 A). We tested the park-luc construct in comparison to the ATF4RE-luc construct under ER stress conditions and observed that luciferase expression from both reporter constructs was increased to a similar extent under ER stress, while the mutant park-luc construct behaved like the pGL3-luc vector control, both in HEK293T and SH-SY5Y cells (Fig. 3 B).

Of note, CCCP treatment also induced increased transcription from both the ATF4RE-luc and the park-luc reporter construct (Supplemental Fig. 1 A, B). Moreover, forced expression of ATF4 or upstream PERK also activated transcription from the park-luc construct (Fig. 3 C). In line with this observation, dominant negative ATF4ΔN, which lacks the N-terminal transcriptional activation domain (44), significantly interfered with the ER stress-induced activation of park-luc (Fig. 3 D).

To increase experimental evidence for a role of endogenous ATF4 in mediating the transcriptional up-regulation of parkin under ER stress, we knocked down ATF4 expression by RNA interference. SH-SY5Y cells were transfected with ATF4 siRNA or control siRNA and the efficiency of the ATF4 knockdown was verified at the ATF4 mRNA and protein level (Fig. 4 A, right panel). Of note, ATF4 is specifically induced after ER stress, while under non-stress conditions ATF4 expression levels are low. Remarkably, in ATF4-deficient cells the up-regulation of parkin induced by ER stress (thapsigargin) or mitochondrial stress (CCCP) was significantly reduced (Fig. 4 A, left panel). The same results were obtained employing two different ATF4-specific siRNA duplexes (data not shown). Moreover, we analyzed the transcriptional regulation of parkin in primary cortical neurons derived from ATF4 knockout mice (45). The up-regulation of parkin in response to the ER stressor tunicamycin was significantly reduced in ATF4-deficient primary neurons (Fig. 4 B), indicating that ATF4 indeed plays an important role in the stress-induced regulation of parkin gene expression. Interestingly, in our experimental approach a transient downregulation of ATF4 had a more severe effect on the stress-induced up-regulation of parkin than a stable knockout of ATF4. It is conceivable that compensatory effects in ATF4 knockout mice account for this observation. The lack of ATF4 from early embryogenesis could induce differential regulation of other transcription factors of the ATF/CREB family members, which partly can compensate for a loss of ATF4 function.

Finally, binding of ATF4 to the parkin promoter could be demonstrated by chromatin immunoprecipitation (ChIP) assays using a polyclonal anti-ATF4 antibody. A rabbit polyclonal antibody against chicken IgG was used as nonspecific control. After isolation of cross-linked chromatin from cells incubated with or without 300 nM thapsigargin, immunoprecipitated DNA was analyzed by real time PCR. The ChIP analysis revealed specific binding of ATF4 to the parkin promoter after 2 and 8 hours of thapsigargin treatment in HEK293T as well as SH-SY5Y cells (Fig. 4 C).

c-Jun acts as a transcriptional repressor of parkin and has a dominant effect on ATF4

When we performed electrophoretic mobility shift assays (EMSAs) using the putative ATF4-binding site of the parkin promoter as a radiolabeled probe (park oligo), we observed a second complex in addition to the ATF4-DNA complex. This complex showed a reduced electrophoretic mobility in comparison to the ATF4-park oligo complex and its relative intensity was increased after ER stress (Fig. 5 A, lanes 1, 2). By testing various antibodies against transcription factors which in principle could bind to the CREB/ATF site for their potential to supershift the upper band, we found that c-Jun is also able to bind to the park oligo. The respective band was supershifted by an anti-c-Jun antibody (Fig. 5 A, lane 3) and was competed by an excess of unlabeled park oligo (Fig. 5 A, lane 5). To test whether c-Jun might have an impact on the transcriptional regulation of parkin expression, we first analyzed the effect of c-Jun on the park-luc reporter construct. Interestingly, increased levels of c-Jun significantly reduced transcription from the park-luc construct under ER stress (Fig. 5 B). Moreover, c-Jun suppressed ATF4-induced activation of park-luc, both under basal and ER stress conditions, indicating a dominant negative effect (Fig. 5 C). Next we performed a c-Jun knockdown approach by RNA interference. c-Jun-specific siRNA duplexes were transfected into SH-SY5Y cells, resulting in a reduction of c-Jun mRNA of ~ 87% under normal conditions and ~ 69% under ER stress conditions (Supplemental Fig. 2). The knockdown

efficiency was also verified at the protein level (Fig. 5 D, lower panel). Notably, in c-Jun-deficient cells parkin up-regulation in response to ER stress was significantly increased and also in non-stressed cells a higher parkin expression was observed when c-Jun was silenced (Fig. 5 D, upper panel). These results indicate that c-Jun can bind to the ATF4-binding site within the parkin promoter to mediate repression of parkin gene expression. c-Jun is a major target of JNKs (c-Jun N-terminal kinases), a subfamily of the mitogen-activated protein kinase (MAPK) superfamily. JNK1 and JNK2 are ubiquitously expressed, while JNK3 is primarily found in brain, heart and testes (rev. in (46-48). Since JNK3 has been linked to cell death in several models of neurodegeneration (rev. in (49, 50), we tested whether it has an impact on parkin gene expression. Increased expression of JNK3 indeed significantly suppressed transcription from the park-luc construct (Fig. 5 E). Moreover, treatment of cells with the JNK inhibitor SP600125 increased parkin mRNA and protein levels both under stress and non-stress conditions (Fig. 5 F).

Parkin protects cells from ER stress-induced cell death

Conceptually, up-regulation of parkin expression in response to ER stress might help to preserve cellular function and survival within the adaptive phase of the UPR. To test the capacity of parkin to protect cells from ER stress-induced toxicity, we treated SH-SY5Y cells transiently expressing wildtype (wt) parkin or pathogenic parkin mutants with thapsigargin or tunicamycin. Cells undergoing apoptosis were analyzed by indirect fluorescence using an antibody specific for activated caspase-3. In contrast to control cells and cells expressing parkin mutants associated with autosomal recessive parkinsonism, cells overexpressing wt parkin were protected against cell death induced by ER stress (Fig. 6 A). To increase evidence for a role of endogenous parkin in coping with ER stress, we analyzed the consequences of a parkin knockdown induced by RNA interference. Parkin knockdown cells showed a significant increase in apoptotic cells after ER stress in comparison with control siRNA-

transfected cells (Fig. 6 B). A decrease in the viability of parkin-deficient SH-SY5Y and HEK293T cells after ER stress was also observed by employing the MTT assay (Supplemental Fig. 3 A, B). Notably, the increased vulnerability of parkin-deficient cells to ER stress-induced cell death could be rescued by the expression of siRNA-resistant wt parkin, confirming a parkin-specific effect (Fig. 6 B). In addition, we analyzed the viability of mouse embryonic fibroblasts (MEFs) derived from parkin knockout mice (51) under ER stress conditions. In comparison to MEFs derived from wildtype mice the parkin knockout MEFs showed a decreased viability under ER stress induced by thapsigargin (Fig. 6 C). Moreover, primary skin fibroblasts from three patients with mutations in the parkin gene displayed a significant increase in cell death in response to tunicamycin treatment compared to age- and gender-matched control fibroblasts from healthy individuals (Fig. 6 D). Of note, levels of CHOP, phospho-c-Jun and phospho-JNK, which have been associated with the with the pro-apoptotic branch of ER stress pathways, were increased in patient fibroblasts under ER stress (Supplemental Fig. 4).

Parkin does not decrease the level of ER stress and functions independently from the proteasome

The experiments described above established a protective role of parkin in response to ER stress. To address the question of whether parkin may have an effect on the severity of ER stress, we quantified the mRNA expression of the ER chaperone protein BiP by RT-PCR in parkin knockdown cells in response to ER stress. After ER stress induced by thapsigargin BiP mRNA was highly up-regulated (~15-fold compared to untreated cells). Interestingly, downregulation of parkin had no significant impact on BiP mRNA levels, both under basal conditions and ER stress (Fig. 7 A). In addition, MEFs derived from parkin knockout mice did not show increased levels of BiP mRNA after thapsigargin or tunicamycin treatment when compared to control MEFs (Fig. 7 B). Moreover, BiP mRNA levels in parkin knockout MEFs

were unchanged under non-stressed conditions (data not shown). These results indicated that the transient or stable loss of parkin function does not cause ER stress. In line with these results, increased expression of parkin did not significantly influence the level of ER stress as monitored by luciferase reporter assays using four different ER stress-responsive elements (ESRE, ERSE-II, UPR and ATF4RE), which cover all branches of the UPR (Fig. 7 C and Supplemental Fig. 5). In a next step we tested whether the protective activity of parkin under ER stress is dependent on the proteasome. SH-SY5Y cells were exposed to thapsigargin in the presence of the proteasomal inhibitor epoxomycin. First, we used a non-toxic concentration of epoxomycin (0.1 μM), which efficiently inhibited the proteasome, as shown by an increase in endogenous p53 levels and an accumulation of ubiquitylated proteins (Fig. 7 D). Notably, the efficiency of parkin to protect against ER stress-induced cell death was not impaired when the proteasome was inhibited. Furthermore, increasing parkin expression also prevented cell death induced by a toxic concentration of epoxomycin (10 μM), indicating that protein degradation via the proteasome is not required for the pro-survival effect of parkin (Fig. 7 E).

Parkin interferes with ER stress-induced mitochondrial damage

Obviously, parkin does not reduce ER stress *per se*, but it can protect cells from ER stress-induced cell death. Based on the fact that parkin has an impact on mitochondrial integrity (52), we analyzed the effect of ER stress on mitochondrial morphology and determined whether parkin might play a role in this pathway. SH-SY5Y cells treated with either tunicamycin or thapsigargin were incubated with the fluorescent dye DiOC6(3) to visualize mitochondria in living cells by fluorescence microscopy. Under normal conditions when mitochondrial fusion and fission activities are balanced, cells show a tubular mitochondrial network (rev. in (53-56). When fission is increased relative to fusion, small rod-like or spherical mitochondria can be observed, which are classified as fragmented. An increase in fusion relative to fission results in elongated, highly connected mitochondria.

Typically, about 70% of SH-SY5Y cells show a tubular mitochondrial network under normal conditions, the remaining 30% are characterized by fragmented mitochondria (52, 57). ER stress induced by either tunicamycin or thapsigargin increased the percentage of cells with fragmented mitochondria up to 60% after 5 hours or 70% after 16 hours ER stress (Fig. 8 A). Remarkably, increased expression of parkin significantly reduced ER stress-induced mitochondrial fragmentation (Fig. 8 A, B). Moreover, we observed that parkin loss of function increases the vulnerability of cells to ER stress-induced mitochondrial damage since the cellular ATP production in response to ER stress induced by tunicamycin was significantly reduced in parkin-deficient SH-SY5Y (Fig. 8 C). Thus, parkin maintains mitochondrial integrity under ER stress and prevents alterations in mitochondrial morphology and bioenergetics.

Discussion

A characteristic feature of PD is a strong pathogenic influence by extrinsic and intrinsic cellular stressors. Environmental toxins, such as paraquat, rotenone and manganese increase the risk to develop PD, and the accidental intoxication of young drug addicts with MPTP in the early 1980s strikingly demonstrated that a toxin is able to cause irreversible parkinsonism. A common feature of these toxins is that they damage mitochondria, increase reactive oxygen species (ROS) production and cause ER stress. Intrinsic stress in dopaminergic neurons arises from the enzymatic and non-enzymatic metabolism of dopamine, leading to the generation of ROS. Another source of endogenous stress is excitotoxicity involving overstimulation of glutamate receptors in the substantia nigra. Intriguingly, oxidative stress, excitotoxicity and ER stress are closely linked (28, 58-60), suggesting that both mitochondria and the ER are crucial organelles implicated in the pathogenesis of PD and other neurodegenerative diseases.

In this study we show that parkin is transcriptionally up-regulated by mitochondrial and ER stress via the UPR to promote viability under cellular stress. We identified the transcription factor ATF4 as a key player in the stress-induced regulation of parkin expression which binds to a CREB/ATF site within the parkin promoter. An essential role for ATF4 in the regulation of parkin expression was substantiated by the following observations: First, a dominant negative ATF4 mutant prevented ER stress-induced up-regulation of parkin. Second, in ATF4 knockdown cells and primary neurons from ATF4 knockout mice, parkin up-regulation in response to ER stress was significantly impaired. Finally, we could demonstrate by a ChIP assay that ATF4 indeed binds to the parkin promoter. Our analysis also revealed that c-Jun acts as a transcriptional repressor of parkin. Intriguingly, c-Jun can bind to the same site within the parkin promoter as ATF4 to induce downregulation of parkin expression. What might be the physiological relevance of this observation? Conceptually, c-

Jun may terminate the ATF4-mediated up-regulation of parkin expression by competing with ATF4 on the parkin promoter. In line with this scenario, we observed that c-Jun has a dominant effect on ATF4; it can suppress ATF4-mediated up-regulation of parkin expression. It is also conceivable that severe or prolonged ER stress leads to a preferential binding of c-Jun to the parkin promoter in order to suppress cytoprotective pathways and to favor the elimination of irreversibly damaged cells by pro-apoptotic pathways. In support of this view, CHOP, a pro-apoptotic transcription factor activated upon severe or prolonged ER stress, suppressed parkin expression (Supplemental Fig. 6). Parkin transcription was also repressed by JNK3, a kinase upstream of c-Jun, which has been implicated in neuronal cell death pathways in dopaminergic neurons (61-65). Indeed, our data show that the use of a JNK inhibitor is able to increase the expression of parkin, particularly under stress conditions. Interestingly, parkin has been reported to suppress JNK activity in cellular models and *Drosophila melanogaster* (66-70). In line with these studies, we observed that phospho-JNK and phospho-c-Jun levels are increased in parkin-deficient patient fibroblasts under ER stress (Supplemental Fig. 4) Our finding that the JNK pathway can negatively regulate parkin gene expression suggests a reciprocal interaction between parkin and JNK3, which might be instrumental in the dichotomy of cell survival and death. Depending on the cellular context and the severity of stress conditions, parkin can shift the balance towards cell survival by attenuating JNK3 signaling, while JNK3 gaining the upper hand suppresses pro-survival pathways, either directly or indirectly, for example by inhibiting the expression of parkin.

The increased expression of parkin in response to ER stress clearly serves a cytoprotective function. Cells overexpressing wildtype but not mutant parkin are protected against ER stress-induced cell death, while parkin-deficient cells show an increased vulnerability to ER stress. It will now be interesting to determine which cell types are affected in their response to stress by the loss of parkin function. Based on the emerging concept of non-cell autonomous cell death in neurodegeneration it is conceivable that an impaired stress

response in glial cells in the neighborhood of dopaminergic cells can contribute to nigrostriatal degeneration.

Neither an acute nor a permanent loss of parkin function *per se* causes ER stress. Furthermore, increased parkin expression does not decrease the severity of ER stress, arguing against a direct role of parkin in the ERAD (ER-associated degradation) pathway. In support of this notion, the protective activity of parkin is independent of the proteasome. We observed that proteasomal inhibition does not impair the ability of parkin to prevent ER stress-induced cell death. Which activity of parkin may then be responsible for its protective effect under ER stress? In this context it is important to note that organellar stress within cells cannot be regarded in an isolated manner. In fact, our study adds evidence for an interaction between the ER and mitochondria in response to stress (71). ER stress induced by tunicamycin or thapsigargin causes mitochondrial stress, resulting in a bioenergetic deficit and mitochondrial fragmentation. Our working model would suggest that, at this interplay, parkin seems to enter the stage, preventing the pathophysiological consequences of ER stress on mitochondrial integrity (Fig. 9). The next important step will be to figure out what the precise role of parkin might be in the communication between the ER and mitochondria. A key player in this inter-organellar crosstalk is calcium since mitochondrial uptake of calcium that has been released from the ER can stimulate metabolic activity and increase ATP production (rev. in (32, 72). However, a massive and/or prolonged accumulation of calcium leads to a mitochondrial calcium overload and triggers cell death. Interestingly, it has recently been reported that loss of PINK1, another PD-associated gene which seems to be functionally linked to parkin, leads to mitochondrial calcium overload (73). Parkin can compensate for PINK1 deficiency in different models, thus, it is tempting to speculate that parkin can prevent mitochondrial calcium overload and/or its consequences.

Materials and methods

DNA constructs

The following constructs were described previously: wild-type (wt) human parkin, G430D, ΔUBL mutant parkin (34, 74, 75), ATF4 (76), ATF4ΔN (44), PERK (77), c-Jun (78), JNK3 (79), Bcl-2-FLAG (80), and mCherry (52, 81). To generate siRNA-resistant parkin four silent mutations were introduced into human wt parkin, in order to prevent binding of parkin-specific siRNA1 (Invitrogen, Karlsruhe, Germany). The following mutations were introduced by standard PCR cloning techniques: C 1038 to T, G 1044 to A, C 1053 to A and A 1059 to G. The luciferase reporter constructs were cloned by subcloning the unfolded protein response element (UPRE) (82), the ER stress response element (ERSE) (83), the ER stress response element II (ERSE-II) (84), the ATF4 binding site of the IGFBP-1 promoter (ATF4RE) (43) or the ATF4 binding element of the parkin promoter (PARK) in triplicate flanked by NheI and BglII restriction sites into the pGL3 promoter vector (Promega, Mannheim, Germany). To generate the renilla luciferase construct, the SV40 promoter from the pGL3 vector was subcloned into the phRL-TK vector (Promega), thereby replacing the HSV-TK promoter. The plasmids encoding enhanced yellow fluorescent protein (EYFP) and enhanced green fluorescent protein (cGFP) were purchased from Clontech (Mountain View, CA, USA).

Cell culture and transfections

SH-SY5Y (DSMZ number ACC 209) and HEK293T (ATCCC number CRL-1573) cells were transfected with Lipofectamine Plus (Invitrogen) according to the manufacturer's instructions. For RNA interference, SH-SY5Y or HEK293T cells were reversely transfected with Stealth small interfering RNA (siRNA) (Invitrogen) using Lipofectamine RNAiMAX (Invitrogen) for the SH-SY5Y cells and Lipofectamine 2000 (Invitrogen) for the HEK293T cells.

Antibodies and reagents

The following antibodies were used: anti-parkin mouse monoclonal antibody (mAb) PRK8 (Millipore, Schwalbach, Germany), anti-parkin polyclonal antibody (pAb) 2132, anti-ubiquitin P4D1 pAb (Cell Signaling Technology, Danvers, MA, USA), anti-SAPK/JNK pAb, anti-phospho-SAPK/JNK (Thr183/Tyr185) pAb, anti-phospho-c-Jun (Ser63) II rabbit pAb (Cell Signaling Technology, Danvers, MA, USA), anti-CHOP mAb (Santa Cruz Biotechnology, Santa Cruz, CA, USA), anti-β-actin mAb, anti-Flag M2 mAb, and anti-myc 9E10 mAb (Sigma, Taufkirchen, Germany), anti-c-Jun (N) sc45 rabbit pAb, anti-c-Jun (N) sc45X rabbit pAb, anti-CREB-2 C-20 rabbit pAb, and anti-TRAF6 (H-274) rabbit pAb (Santa Cruz Biotechnology, Santa Cruz, CA, USA), anti-ATF4 pAB (Cocalico Biologicals, Reamstown, PA, USA),), anti-p53 mAb (Calbiochem/Merck, Darmstadt, Germany), anti-active caspase-3 rabbit pAb (Promega), Alexa 555-conjugated goat anti-rabbit pAb (Sigma), horseradish peroxidase (HRP)-conjugated anti-mouse, and anti-rabbit IgG antibody (Promega). Thapsigargin was purchased from Sigma, tunicamycin from Fluka/Sigma (Taufkirchen, Germany), epoxomycin from Calbiochem, L-histidinol from Sigma, the JNK inhibitor SP600125 from Enzo Life Sciences (Loerrach, Germany), dialysed FCS and 3,3'-dihexyloxacarbocyanine iodide (DiOC6(3)) from Invitrogen. The mounting medium Mowiol (Calbiochem) was supplemented with 4', 6-diamidimo-2-phenylindole (DAPI; Sigma).

Western blot analysis

SDS-PAGE and Western blotting was described earlier (34). Antigens were detected with the enhanced chemiluminescence (ECL) detection system (Amersham Biosciences, Freiburg, Germany) or the Immobilon Western chemoluminiscent HRP substrate (Millipore).

Mouse embryonic fibroblast cultures

Primary mouse fibroblasts were isolated from parkin knockout and wildtype mice with the same genetic background (51). E12.5 mouse embryos were extracted and the head and inner organs were removed. The remaining tissue was dissociated by trypsination and trituration.

Primary cortical neuronal culture

Cortical neurons were cultured from wildtype or ATF4 transgenic mouse embryos at E14.5-E15.5 days of gestation and individually dissected. Briefly, neurons from each embryo were plated individually, into six-well dishes (~3 million cells/well) coated with poly-D-lysine (100 μg/ml) in serum-free medium [MEM/F12 (1:1) supplemented with 6 mg/ml D-glucose, 100 μg/ml transferrin, 25 μg/ml insulin, 20 nM progesterone, 60 μM putrescine, 30 nM selenium] as described previously (85). At 2 days in vitro cortical neurons were treated with tunicamycin (3 μg/ml) for 8 h. Stock solutions of tunicamycin were prepared in DMSO (all from Sigma Aldrich, Oakville, ON, Canada) and diluted in culture media immediately prior to addition. Total RNA was isolated from cells at indicated time points using Trizol reagent as per manufacturers' instructions (Invitrogen). RNA concentrations were measured on a spectrophotometer at λ260nm.

Human primary fibroblast cultures

Punch skin biopsies were taken from PD patients with compound heterozygous mutations (c101delAG, het. del ex3/4; patients 1 and 2) or a heterozygous mutation (het. dupl. ex7; patient 3) in the parkin gene. Genotyping was performed using direct DNA sequencing and the Multiplex ligation-dependent probe amplification parkin gene dosage kits (P051; MRC-Holland, Amsterdam, Holland), covering all exons of the parkin gene, as well as other known Mendelian PD genes. Sex and age-matched control fibroblasts from healthy individuals were provided by the Department of Orthopedics (Universitätsklinik für Orthopädie, Eberhard Karls University, Tübingen, Germany). Chopped tissue pieces were placed into a tissue culture flask and carefully covered with maintenance medium (RPMI medium supplemented with 10% fetal bovine serum and 1% penicillin/streptomycin, 1 mM sodium pyruvate). Cultures were kept at 37°C in a humidified atmosphere containing 5% CO2. Harvested fibroblasts were aliquoted and frozen for storage between passages 2 and 10.

Real-Time RT-PCR

Real-Time RT-PCR was performed, as described before (34). Briefly, SH-SY5Y cells were

incubated with 1 µM thapsigargin or 2 µg/ml tunicamycin, 10 µM CCCP or 10 µM SP600125 for the indicated time. Total cellular RNA was isolated according to manufacturer's instructions (RNaesy mini kit, QIAGEN, Hilden , Germany). cDNA was synthesized using iScript cDNA Synthesis Kit (Bio-Rad, München, Germany). For the quantification of human parkin mRNA the TaqMan Gene Expression Assay (parkin: Hs01038827-m1; beta actin: P/N 4326315E; 18sRNA: P/N 4319413E) (Applied Biosystems, Foster City, CA, USA) was used. For all other mRNA quantifications, PCR reactions were performed with 2x Power SYBR Green PCR Master Mix (Applied Biosystems) and 1 µM of each primer pair; mouse (m) parkin forward primer (F): 5'-AAA CCG GAT GAG TGG TGA GT-3'; m-parkin reverse primer (R): 5'-AGC TAC CGA CGT GTC CTT GT-3'; m-actin-β F: 5'-AGC CTT CCT TCT TGG GTA TG-3'; m-actin-β R: 5'-GGT CTT TAC GGA TGT CAA CG-3'; m-BiP F: 5'-GCC TCA TCG GAC GCA CTT-3'; m-BiP R: 5'-GGG GCA AAT GTC TTG GTT-3'; human (h) ATF4: F: 5'-CCC TTC ACC TTC TTA CAA CCT C-3'; h-ATF4 R: 5'-GTC TGG CTT CCT ATC TCC TTC A-3'; h-c-Jun F 5'-CGC CTG ATA ATC CAG TCC A-3'; h-c-Jun R: 5'-CCT GCT CAT CTG TCA CGT TC-3' ; h-BIP F: 5'-GCT CGA CTC GAA TTC CAA AG-3'; h-BIP R: 5'-GAT CAC CAG AGA GCA CAC CA-3'; h-actin-β F: 5'-TGG ACT TCG AGC AAG AGA TG-3'; h-actin-β R: 5'-AGG AAG GAA GGC TGG AAG AG-3').
Quantification was performed with 7500 Fast Real Time System (Applied Biosystems) based on triplicates per primer set. Gene expression was normalized with respect to endogenous housekeeping control genes, β-actin and 18sRNA, which were not influenced by ER stress. Relative expression was calculated for each gene using the $\Delta\Delta C_T$ method. Statistical analysis of RT-PCR data is based on at least three independent experiments with tripicates samples.

Luciferase Assays

HEK293T or SH-SY5Y cells transiently expressing renilla luciferase and firefly luciferase reporter plasmids were subjected to the stress treatment indicated. Luciferase activity of cell

lysates was determined luminometrically using an LB96V luminometer (Berthold Technologies, Bad Wildbad, Germany) by the dual luciferase assay system (Promega) as specified by the manufacturer. The measured values were analyzed with WinGlow Software (Berthold Technologies). Quantification was based on at least three independent experiments. Per experiment, each transfection was performed at least in triplicate.

Apoptosis and cell viability assays

Activation of caspase-3 was determined as described previously (80). Briefly, SH-SY5Y cells or skin fibroblasts were grown on glass coverslips. 24 h after transfection (for parkin knockdown three days later), cells were incubated with thapsigargin, tunicamycin and/or epoxomycin as indicated. The cells were then fixed and activated caspase-3 detected by indirect immunofluorescence using an anti-active caspase-3 antibody. To detect cells undergoing apoptosis, the number of activated caspase-3-positive cells out of at least 300 transfected cells was determined using a Zeiss Axioscope 2 plus microscope (Carl Zeiss, Göttingen, Germany). Quantifications were based on triplicates of at least three (SH-SY5Y cells) or two (human skin fibroblasts) independent experiments. Per experiment ≥ 300 cells per coverslip of triplicate samples were assessed. For the cell viability assays SH-SY5Y cells, HEK293T cells or mouse embryonic fibroblasts were plated into 12 well plates. SH-SY5Y cells and HEK293T cells were reversely transfected with parkin or control siRNA. 2 days later the cells were stressed with tunicamycin or thapsigargin as indicated and the Vybrant MTT Cell Proliferation Assay was performed according to manufacturer's instructions (Invitrogen).

Electrophoretic mobility shift assay

Nuclear extracts were prepared as described earlier (34). For the binding reaction 10 µg of extracts were incubated with 10 mM HEPES (pH 7.9), 50 mM NaCl, 5 mM $MgCl_2$, 2 mM DTT, 0.1 mM EDTA, 5% glycerol, 10 µg BSA, 2 µg poly(dI-dC) and 0.2 ng (20,000 cpm) of ^{32}P-labeled, double-stranded park oligonucleotide (5'-CCCCGGTGACGTAAGATTGC-3')

in a final volume of 20 µl. For supershift assays 0.2 µg of the ATF4 antibody or 2 µg of the c-Jun (N) sc45X antibody, for competition experiments 50 ng (100x) of cold park oligonucleotide was added to the binding reaction. After binding on ice for 30 min, mixtures were loaded onto nondenaturating 4% polyacrylamide gels in 0.5 x TBE (45 mM Tris borate and 1 mM EDTA). Gels were electrophoresed at 4°C for 4 h at 160V, dried, and exposed for autoradiography at -80°C.

Chromatin immunoprecipitation (ChIP)

HEK293T or SH-SY5Y cells were replenished with fresh medium 12 h prior to initiating all treatments to ensure that the cells were in the basal state. To trigger the UPR, fresh medium containing 300 nM thapsigargin was added. To monitor ATF4 binding to the parkin gene, a ChIP assay was performed as previously described (86). The ATF4 antibody was a rabbit polycolonal antibody. DNA enrichment at the parkin promoter region that contains the potential ATF4 binding site was analyzed with quantitative real time PCR. A 5 µl aliquot of DNA was mixed with 62.5 pmol of each PCR primer and 12.5 µl of SYBR Green PCR master mix (Applied Biosystems) in a 25 µl total volume. The real-time PCR was performed with a DNA Engine Opticon 3 system (Bio-Rad). The reaction mixtures were incubated at 95°C for 15 min, followed by amplification at 95°C for 15 s and 60°C for 60 s for 35 cycles. All experiments were performed in triplicate and each sample was subjected to PCR in duplicate. The primers used were: forward: 5'-GTTGCTAAGCGACTGGTCAA-3' and reverse: 5'-CAGCCCCCCACCGCCGCC-3'.

Flourescent staining of mitochondria

SH-SY5Y cells were grown on 15 mm glas coverslips, and were fluorescently labeled with 0.1 µM DiOC6(3) in cell culture medium for 15 min. After washing coverslips with medium, living cells were analyzed for mitochondrial morphology by fluorescence microscopy as described previously (52) using a Leica DMRB microscope (Leica, Wetzlar, Germany). Cells were categorized in two classes according to their mitochondrial morphology: tubular or

fragmented. Quantifications were based on three independent experiments. Per experiment the mitochondrial morphology of ≥ 300 transfected cells per coverslip of triplicate samples was assessed.

Measurement of cellular ATP levels

A quantitative determination of ATP in SH-SY5Y cells was performed using the ATP Bioluminescence Assay Kit HS II (Roche, Mannheim, Germany) according to the manufacturer's instructions. Briefly, SH-SY5Y cells were reversely transfected with the indicated siRNA duplexes. 24 h prior to harvesting the culture medium was replaced by low glucose medium containing 3 mM instead of 25 mM glucose. 5 h before the measurement cells were treated with 2 µg/ml tunicamycin. Cells were washed twice with PBS, scraped of the plate and then lysed according to the provided protocol. ATP content of the samples was determined using an LB96V luminometer (Berthold Technologies), analyzed with WinGlow Software (Berthold Technologies) and normalized to total protein levels. Quantification was based on at least three independent experiments. Per experiment, each transfection was performed at least in triplicate.

Bioinformatics

Transcription factor (TF) binding sites were identified by the TFSEARCH (40) and the MatInspector (87) program. All sequences were derived from the promoter sequence retrieval database ElDorado 02-2010 (Genomatix, Munich/Germany). Promoter sequences of parkin from four different mammalian species were aligned with the DiAlign TF program (87) in the Genomatix software suite GEMS Launcher to evaluate overall promoter similarity and to identify conserved CREB/ATF binding sites (BSs). The promoter sequences were defined as in ElDorado and elongated at the 3' end of the promoter (downstream) by 150 base pairs. Position weight and matrices were used according to Matrix Family Library Version 8.2 (January 2010) for promoter analyses. BSs were considered as "conserved BSs" if the

promoter sequences of human and the orthologs can be aligned in the region of CREB/ATF BSs with the help of the DiAlign TF program (using default settings).

Statistical analysis

Data were expressed as means ± SE. Statistical analysis was carried out using ANOVA. *$p < 0.05$, **$p < 0.01$, ***$p < 0.001$.

Acknowledgements

This work was supported by the Deutsche Forschungsgemeinschaft (SFB 596 "Molecular Mechanisms of Neurodegeneration" to KFW, JT, and WW), the German Ministry for Education and Research (NGFN plus "Functional Genomics of Parkinson's Disease" to KFW, TG and WW), the Helmholtz Alliance “Mental Health in an Ageing Society” (to KFW, TG and WW), the Hans and Ilse Breuer Foundation (to LB), the Heart and Stroke Foundation of Canada, Heart and Stroke Foundation of Ontario, and the Canadian Institutes of Health Research (to DSP). Funding for MSK was from the National Institutes of Health (DK-52064). II was supported by a postdoctoral fellowship from Canadian Institutes of Health Research (CIHR).We are grateful to Christian Haass for continuous support and stimulating discussions. We thank Drs. Tim Townes for providing the ATF4 knockout mice, Alexis Brice and Olga Corti for the parkin knockout mice, Torsten Kluba for human skin fibroblasts from control individuals, Carsten Culmsee for primary mouse cortical neurons, Daniel Krappmann for the c-Jun plasmid, Kimitoshi Kohno and Hiroto Izumi for the ATF4 plasmid, Gerald Thiel for the ATF4ΔN and CHOP plasmids, David Ron for the PERK plasmid, and Vicky Wätzig and Thomas Herdegen for the JNK3 plasmid. We thank Kerstin Lämmermann and Christian Naumann for technical assistance and Jonathan Lin for advice on ATF4 Western blotting.

Supplementary information is available at Cell Death & Differentiation's website.

References

1. Winklhofer KF, Haass C. Mitochondrial dysfunction in Parkinson's disease. Biochim Biophys Acta. 2010 Jan;1802(1):29-44.

2. Schapira AH. Mitochondria in the aetiology and pathogenesis of Parkinson's disease. Lancet Neurol. 2008 Jan;7(1):97-109.

3. Bueler H. Impaired mitochondrial dynamics and function in the pathogenesis of Parkinson's disease. Exp Neurol. 2009 Mar 18.

4. Wang HQ, Takahashi R. Expanding insights on the involvement of endoplasmic reticulum stress in Parkinson's disease. Antioxid Redox Signal. 2007 May;9(5):553-561.

5. Lindholm D, Wootz H, Korhonen L. ER stress and neurodegenerative diseases. Cell Death Differ. 2006 Mar;13(3):385-392.

6. Conn KJ, Gao W, McKee A, Lan MS, Ullman MD, Eisenhauer PB, Fine RE, Wells JM. Identification of the protein disulfide isomerase family member PDIp in experimental Parkinson's disease and Lewy body pathology. Brain Res. 2004 Oct 1;1022(1-2):164-172.

7. Ghribi O, Herman MM, Pramoonjago P, Savory J. MPP+ induces the endoplasmic reticulum stress response in rabbit brain involving activation of the ATF-6 and NF-kappaB signaling pathways. J Neuropathol Exp Neurol. 2003 Nov;62(11):1144-1153.

8. Ryu EJ, Harding HP, Angelastro JM, Vitolo OV, Ron D, Greene LA. Endoplasmic reticulum stress and the unfolded protein response in cellular models of Parkinson's disease. J Neurosci. 2002 Dec 15;22(24):10690-10698.

9. Ryu EJ, Angelastro JM, Greene LA. Analysis of gene expression changes in a cellular model of Parkinson disease. Neurobiol Dis. 2005 Feb;18(1):54-74.

10. Holtz WA, O'Malley KL. Parkinsonian mimetics induce aspects of unfolded protein response in death of dopaminergic neurons. J Biol Chem. 2003 May 23;278(21):19367-19377.

11. Holtz WA, Turetzky JM, Jong YJ, O'Malley KL. Oxidative stress-triggered unfolded protein response is upstream of intrinsic cell death evoked by parkinsonian mimetics. J Neurochem. 2006 Oct;99(1):54-69.

12. Holtz WA, Turetzky JM, O'Malley KL. Microarray expression profiling identifies early signaling transcripts associated with 6-OHDA-induced dopaminergic cell death. Antioxid Redox Signal. 2005 May-Jun;7(5-6):639-648.

13. Yamamuro A, Yoshioka Y, Ogita K, Maeda S. Involvement of endoplasmic reticulum stress on the cell death induced by 6-hydroxydopamine in human neuroblastoma SH-SY5Y cells. Neurochem Res. 2006 May;31(5):657-664.

14. Cooper AA, Gitler AD, Cashikar A, Haynes CM, Hill KJ, Bhullar B, Liu K, Xu K, Strathearn KE, Liu F, Cao S, Caldwell KA, Caldwell GA, Marsischky G, Kolodner RD, Labaer J, Rochet JC, Bonini NM, Lindquist S. Alpha-synuclein blocks ER-Golgi traffic and Rab1 rescues neuron loss in Parkinson's models. Science. 2006 Jul 21;313(5785):324-328.

15. Smith WW, Jiang H, Pei Z, Tanaka Y, Morita H, Sawa A, Dawson VL, Dawson TM, Ross CA. Endoplasmic reticulum stress and mitochondrial cell death pathways mediate A53T mutant alpha-synuclein-induced toxicity. Hum Mol Genet. 2005 Dec 15;14(24):3801-3811.

16. Sugeno N, Takeda A, Hasegawa T, Kobayashi M, Kikuchi A, Mori F, Wakabayashi K, Itoyama Y. Serine 129 phosphorylation of alpha-synuclein induces unfolded protein response-mediated cell death. J Biol Chem. 2008 Aug 22;283(34):23179-23188.

17. Hoozemans JJ, van Haastert ES, Eikelenboom P, de Vos RA, Rozemuller JM, Scheper W. Activation of the unfolded protein response in Parkinson's disease. Biochem Biophys Res Commun. 2007 Mar 16;354(3):707-711.

18. Moran LB, Croisier E, Duke DC, Kalaitzakis ME, Roncaroli F, Deprez M, Dexter DT, Pearce RK, Graeber MB. Analysis of alpha-synuclein, dopamine and parkin pathways in neuropathologically confirmed parkinsonian nigra. Acta Neuropathol (Berl). 2007 Mar;113(3):253-263.

19. Imai Y, Soda M, Inoue H, Hattori N, Mizuno Y, Takahashi R. An unfolded putative transmembrane polypeptide, which can lead to endoplasmic reticulum stress, is a substrate of parkin. Cell. 2001;105(7):891-902.

20. Imai Y, Soda M, Takahashi R. Parkin suppresses unfolded protein stress-induced cell death through its E3 ubiquitin-protein ligase activity. J Biol Chem. 2000;275(46):35661-35664.

21. Yang Y, Nishimura I, Imai Y, Takahashi R, Lu B. Parkin suppresses dopaminergic neuron-selective neurotoxicity induced by Pael-R in Drosophila. Neuron. 2003;37(6):911-924.

22. Wang HQ, Imai Y, Inoue H, Kataoka A, Iita S, Nukina N, Takahashi R. Pael-R transgenic mice crossed with parkin deficient mice displayed progressive and selective catecholaminergic neuronal loss. J Neurochem. 2008 Oct;107(1):171-185.

23. Kitada T, Asakawa S, Hattori N, Matsumine H, Yamamura Y, Minoshima S, Yokochi M, Mizuno Y, Shimizu N. Mutations in the parkin gene cause autosomal parkinsonism. Nature. 1998;392(6676):605-608.

24. West AB, Maidment NT. Genetics of parkin-linked disease. Hum Genet. 2004 Mar;114(4):327-336.

25. Ron D, Walter P. Signal integration in the endoplasmic reticulum unfolded protein response. Nat Rev Mol Cell Biol. 2007 Jul;8(7):519-529.

26. Zhang K, Kaufman RJ. Signaling the unfolded protein response from the endoplasmic reticulum. J Biol Chem. 2004 Jun 18;279(25):25935-25938.

27. Bernales S, Papa FR, Walter P. Intracellular signaling by the unfolded protein response. Annu Rev Cell Dev Biol. 2006;22:487-508.

28. Kim I, Xu W, Reed JC. Cell death and endoplasmic reticulum stress: disease relevance and therapeutic opportunities. Nat Rev Drug Discov. 2008 Dec;7(12):1013-1030.

29. Szegezdi E, Logue SE, Gorman AM, Samali A. Mediators of endoplasmic reticulum stress-induced apoptosis. EMBO Rep. 2006 Sep;7(9):880-885.

30. Rutkowski DT, Kaufman RJ. A trip to the ER: coping with stress. Trends Cell Biol. 2004 Jan;14(1):20-28.

31. Xu C, Bailly-Maitre B, Reed JC. Endoplasmic reticulum stress: cell life and death decisions. J Clin Invest. 2005 Oct;115(10):2656-2664.

32. Pizzo P, Pozzan T. Mitochondria-endoplasmic reticulum choreography: structure and signaling dynamics. Trends Cell Biol. 2007 Oct;17(10):511-517.

33. Hayashi T, Rizzuto R, Hajnoczky G, Su TP. MAM: more than just a housekeeper. Trends Cell Biol. 2009 Feb;19(2):81-88.

34. Henn IH, Bouman L, Schlehe JS, Schlierf A, Schramm JE, Wegener E, Nakaso K, Culmsee C, Berninger B, Krappmann D, Tatzelt J, Winklhofer KF. Parkin mediates neuroprotection through activation of IkappaB kinase/nuclear factor-kappaB signaling. J Neurosci. 2007 Feb 21;27(8):1868-1878.

35. Narendra D, Tanaka A, Suen DF, Youle RJ. Parkin is recruited selectively to impaired mitochondria and promotes their autophagy. J Cell Biol. 2008 Dec 1;183(5):795-803.

36. Narendra DP, Jin SM, Tanaka A, Suen DF, Gautier CA, Shen J, Cookson MR, Youle RJ. PINK1 is selectively stabilized on impaired mitochondria to activate Parkin. PLoS Biol. 2010;8(1):e1000298.

37. Vives-Bauza C, Zhou C, Huang Y, Cui M, de Vries RL, Kim J, May J, Tocilescu MA, Liu W, Ko HS, Magrane J, Moore DJ, Dawson VL, Grailhe R, Dawson TM, Li C, Tieu K, Przedborski S. PINK1-dependent recruitment of Parkin to mitochondria in mitophagy. Proc Natl Acad Sci U S A. 2010 Jan 5;107(1):378-383.

38. Geisler S, Holmstrom KM, Skujat D, Fiesel FC, Rothfuss OC, Kahle PJ, Springer W. PINK1/Parkin-mediated mitophagy is dependent on VDAC1 and p62/SQSTM1. Nat Cell Biol. 2010 Feb;12(2):119-131.

39. Kawajiri S, Saiki S, Sato S, Sato F, Hatano T, Eguchi H, Hattori N. PINK1 is recruited to mitochondria with parkin and associates with LC3 in mitophagy. FEBS Lett. 2010 Mar 19;584(6):1073-1079.

40. Heinemeyer T, Wingender E, Reuter I, Hermjakob H, Kel AE, Kel OV, Ignatieva EV, Ananko EA, Podkolodnaya OA, Kolpakov FA, Podkolodny NL, Kolchanov NA. Databases on transcriptional regulation: TRANSFAC, TRRD and COMPEL. Nucleic Acids Res. 1998 Jan 1;26(1):362-367.

41. Cohen CD, Klingenhoff A, Boucherot A, Nitsche A, Henger A, Brunner B, Schmid H, Merkle M, Saleem MA, Koller KP, Werner T, Grone HJ, Nelson PJ, Kretzler M. Comparative promoter analysis allows de novo identification of specialized cell junction-associated proteins. Proc Natl Acad Sci U S A. 2006 Apr 11;103(15):5682-5687.

42. Kozutsumi Y, Segal M, Normington K, Gething MJ, Sambrook J. The presence of malfolded proteins in the endoplasmic reticulum signals the induction of glucose-regulated proteins. Nature. 1988;332(6163):462-464.

43. Marchand A, Tomkiewicz C, Magne L, Barouki R, Garlatti M. Endoplasmic reticulum stress induction of insulin-like growth factor-binding protein-1 involves ATF4. J Biol Chem. 2006 Jul 14;281(28):19124-19133.

44. Steinmuller L, Thiel G. Regulation of gene transcription by a constitutively active mutant of activating transcription factor 2 (ATF2). Biol Chem. 2003 Apr;384(4):667-672.

45. Masuoka HC, Townes TM. Targeted disruption of the activating transcription factor 4 gene results in severe fetal anemia in mice. Blood. 2002 Feb 1;99(3):736-745.

46. Johnson GL, Nakamura K. The c-jun kinase/stress-activated pathway: regulation, function and role in human disease. Biochim Biophys Acta. 2007 Aug;1773(8):1341-1348.

47. Davis RJ. Signal transduction by the JNK group of MAP kinases. Cell. 2000 Oct 13;103(2):239-252.

48. Chang L, Karin M. Mammalian MAP kinase signalling cascades. Nature. 2001 Mar 1;410(6824):37-40.

49. Waetzig V, Herdegen T. Context-specific inhibition of JNKs: overcoming the dilemma of protection and damage. Trends Pharmacol Sci. 2005 Sep;26(9):455-461.

50. Silva RM, Kuan CY, Rakic P, Burke RE. Mixed lineage kinase-c-jun N-terminal kinase signaling pathway: a new therapeutic target in Parkinson's disease. Mov Disord. 2005 Jun;20(6):653-664.

51. Itier JM, Ibanez P, Mena MA, Abbas N, Cohen-Salmon C, Bohme GA, Laville M, Pratt J, Corti O, Pradier L, Ret G, Joubert C, Periquet M, Araujo F, Negroni J, Casarejos MJ, Canals S, Solano R, Serrano A, Gallego E, Sanchez M, Denefle P, Benavides J, Tremp G, Rooney TA, Brice A, Garcia De Yebenes J. Parkin gene inactivation alters behaviour and dopamine neurotransmission in the mouse. Hum Mol Genet. 2003;12(18):2277-2291.

52. Lutz AK, Exner N, Fett ME, Schlehe JS, Kloos K, Lammermann K, Brunner B, Kurz-Drexler A, Vogel F, Reichert AS, Bouman L, Vogt-Weisenhorn D, Wurst W, Tatzelt J, Haass C, Winklhofer KF. Loss of Parkin or PINK1 Function Increases Drp1-dependent Mitochondrial Fragmentation. J Biol Chem. 2009 Aug 21;284(34):22938-22951.

53. Suen DF, Norris KL, Youle RJ. Mitochondrial dynamics and apoptosis. Genes Dev. 2008 Jun 15;22(12):1577-1590.

54. Knott AB, Bossy-Wetzel E. Impairing the mitochondrial fission and fusion balance: a new mechanism of neurodegeneration. Ann N Y Acad Sci. 2008 Dec;1147:283-292.

55. Detmer SA, Chan DC. Functions and dysfunctions of mitochondrial dynamics. Nat Rev Mol Cell Biol. 2007 Nov;8(11):870-879.

56. Chan DC. Mitochondria: dynamic organelles in disease, aging, and development. Cell. 2006 Jun 30;125(7):1241-1252.

57. Sandebring A, Thomas KJ, Beilina A, van der Brug M, Cleland MM, Ahmad R, Miller DW, Zambrano I, Cowburn RF, Behbahani H, Cedazo-Minguez A, Cookson MR.

Mitochondrial alterations in PINK1 deficient cells are influenced by calcineurin-dependent dephosphorylation of dynamin-related protein 1. PLoS ONE. 2009;4(5):e5701.

58. Malhotra JD, Kaufman RJ. Endoplasmic reticulum stress and oxidative stress: a vicious cycle or a double-edged sword? Antioxid Redox Signal. 2007 Dec;9(12):2277-2293.

59. Sokka AL, Putkonen N, Mudo G, Pryazhnikov E, Reijonen S, Khiroug L, Belluardo N, Lindholm D, Korhonen L. Endoplasmic reticulum stress inhibition protects against excitotoxic neuronal injury in the rat brain. J Neurosci. 2007 Jan 24;27(4):901-908.

60. Yu Z, Luo H, Fu W, Mattson MP. The endoplasmic reticulum stress-responsive protein GRP78 protects neurons against excitotoxicity and apoptosis: suppression of oxidative stress and stabilization of calcium homeostasis. Exp Neurol. 1999 Feb;155(2):302-314.

61. Hunot S, Vila M, Teismann P, Davis RJ, Hirsch EC, Przedborski S, Rakic P, Flavell RA. JNK-mediated induction of cyclooxygenase 2 is required for neurodegeneration in a mouse model of Parkinson's disease. Proc Natl Acad Sci U S A. 2004 Jan 13;101(2):665-670.

62. Ries V, Silva RM, Oo TF, Cheng HC, Rzhetskaya M, Kholodilov N, Flavell RA, Kuan CY, Rakic P, Burke RE. JNK2 and JNK3 combined are essential for apoptosis in dopamine neurons of the substantia nigra, but are not required for axon degeneration. J Neurochem. 2008 Dec;107(6):1578-1588.

63. Brecht S, Kirchhof R, Chromik A, Willesen M, Nicolaus T, Raivich G, Wessig J, Waetzig V, Goetz M, Claussen M, Pearse D, Kuan CY, Vaudano E, Behrens A, Wagner E, Flavell RA, Davis RJ, Herdegen T. Specific pathophysiological functions of JNK isoforms in the brain. Eur J Neurosci. 2005 Jan;21(2):363-377.

64. Pan J, Xiao Q, Sheng CY, Hong Z, Yang HQ, Wang G, Ding JQ, Chen SD. Blockade of the translocation and activation of c-Jun N-terminal kinase 3 (JNK3) attenuates dopaminergic neuronal damage in mouse model of Parkinson's disease. Neurochem Int. 2009 Jun;54(7):418-425.

65. Pan J, Wang G, Yang HQ, Hong Z, Xiao Q, Ren RJ, Zhou HY, Bai L, Chen SD. K252a prevents nigral dopaminergic cell death induced by 6-hydroxydopamine through inhibition of both mixed-lineage kinase 3/c-Jun NH2-terminal kinase 3 (JNK3) and apoptosis-inducing kinase 1/JNK3 signaling pathways. Mol Pharmacol. 2007 Dec;72(6):1607-1618.

66. Jiang H, Ren Y, Zhao J, Feng J. Parkin protects human dopaminergic neuroblastoma cells against dopamine-induced apoptosis. Hum Mol Genet. 2004;13(16):1745-1754. Epub 2004 Jun 1715.

67. Ren Y, Jiang H, Yang F, Nakaso K, Feng J. Parkin protects dopaminergic neurons against microtubule-depolymerizing toxins by attenuating microtubule-associated protein kinase activation. J Biol Chem. 2009 Feb 6;284(6):4009-4017.

68. Liu M, Aneja R, Sun X, Xie S, Wang H, Wu X, Dong JT, Li M, Joshi HC, Zhou J. Parkin regulates Eg5 expression by Hsp70 ubiquitination-dependent inactivation of c-Jun NH2-terminal kinase. J Biol Chem. 2008 Dec 19;283(51):35783-35788.

69. Hasegawa T, Treis A, Patenge N, Fiesel FC, Springer W, Kahle PJ. Parkin protects against tyrosinase-mediated dopamine neurotoxicity by suppressing stress-activated protein kinase pathways. J Neurochem. 2008 Jun;105(5):1700-1715.

70. Cha GH, Kim S, Park J, Lee E, Kim M, Lee SB, Kim JM, Chung J, Cho KS. Parkin negatively regulates JNK pathway in the dopaminergic neurons of Drosophila. Proc Natl Acad Sci U S A. 2005 Jul 19;102(29):10345-10350.

71. Hom JR, Gewandter JS, Michael L, Sheu SS, Yoon Y. Thapsigargin induces biphasic fragmentation of mitochondria through calcium-mediated mitochondrial fission and apoptosis. J Cell Physiol. 2007 Aug;212(2):498-508.

72. Rizzuto R, Marchi S, Bonora M, Aguiari P, Bononi A, De Stefani D, Giorgi C, Leo S, Rimessi A, Siviero R, Zecchini E, Pinton P. Ca(2+) transfer from the ER to mitochondria: When, how and why. Biochim Biophys Acta. 2009 Mar 31.

73. Gandhi S, Wood-Kaczmar A, Yao Z, Plun-Favreau H, Deas E, Klupsch K, Downward J, Latchman DS, Tabrizi SJ, Wood NW, Duchen MR, Abramov AY. PINK1-associated Parkinson's disease is caused by neuronal vulnerability to calcium-induced cell death. Mol Cell. 2009 Mar 13;33(5):627-638.

74. Henn IH, Gostner JM, Tatzelt J, Winklhofer KF. Pathogenic mutations inactivate parkin by distinct mechanisms. J Neurochem. 2005;92:114-122.

75. Winklhofer KF, Henn IH, Kay-Jackson P, Heller U, Tatzelt J. Inactivation of parkin by oxidative stress and C-terminal truncations; a protective role of molecular chaperones. J Biol Chem. 2003;278:47199-47208.

76. Tanabe M, Izumi H, Ise T, Higuchi S, Yamori T, Yasumoto K, Kohno K. Activating transcription factor 4 increases the cisplatin resistance of human cancer cell lines. Cancer Res. 2003 Dec 15;63(24):8592-8595.

77. Harding HP, Zhang Y, Ron D. Protein translation and folding are coupled by an endoplasmic-reticulum-resident kinase. Nature. 1999 Jan 21;397(6716):271-274.

78. Krappmann D, Wulczyn FG, Scheidereit C. Different mechanisms control signal-induced degradation and basal turnover of the NF-kappaB inhibitor IkappaB alpha in vivo. Embo J. 1996 Dec 2;15(23):6716-6726.

79. Waetzig V, Herdegen T. A single c-Jun N-terminal kinase isoform (JNK3-p54) is an effector in both neuronal differentiation and cell death. J Biol Chem. 2003 Jan 3;278(1):567-572.

80. Rambold AS, Miesbauer M, Rapaport D, Bartke T, Baier M, Winklhofer KF, Tatzelt J. Association of Bcl-2 with misfolded prion protein is linked to the toxic potential of cytosolic PrP. Mol Biol Cell. 2006;17:3356-3368.

81. Shaner NC, Campbell RE, Steinbach PA, Giepmans BN, Palmer AE, Tsien RY. Improved monomeric red, orange and yellow fluorescent proteins derived from Discosoma sp. red fluorescent protein. Nat Biotechnol. 2004 Dec;22(12):1567-1572.

82. Wang Y, Shen J, Arenzana N, Tirasophon W, Kaufman RJ, Prywes R. Activation of ATF6 and an ATF6 DNA binding site by the endoplasmic reticulum stress response. J Biol Chem. 2000 Sep 1;275(35):27013-27020.

83. Yoshida H, Haze K, Yanagi H, Yura T, Mori K. Identification of the cis-acting endoplasmic reticulum stress response element responsible for transcriptional induction of mammalian glucose-regulated proteins. Involvement of basic leucine zipper transcription factors. J Biol Chem. 1998 Dec 11;273(50):33741-33749.

84. Kokame K, Kato H, Miyata T. Identification of ERSE-II, a new cis-acting element responsible for the ATF6-dependent mammalian unfolded protein response. J Biol Chem. 2001 Mar 23;276(12):9199-9205.

85. Aleyasin H, Cregan SP, Iyirhiaro G, O'Hare MJ, Callaghan SM, Slack RS, Park DS. Nuclear factor-(kappa)B modulates the p53 response in neurons exposed to DNA damage. J Neurosci. 2004 Mar 24;24(12):2963-2973.

86. Chen H, Pan YX, Dudenhausen EE, Kilberg MS. Amino acid deprivation induces the transcription rate of the human asparagine synthetase gene through a timed program of expression and promoter binding of nutrient-responsive basic region/leucine zipper transcription factors as well as localized histone acetylation. J Biol Chem. 2004 Dec 3;279(49):50829-50839.

87. Cartharius K, Frech K, Grote K, Klocke B, Haltmeier M, Klingenhoff A, Frisch M, Bayerlein M, Werner T. MatInspector and beyond: promoter analysis based on transcription factor binding sites. Bioinformatics. 2005 Jul 1;21(13):2933-2942.

Figure Legends

Fig. 1. Mitochondrial stress induced by CCCP activates the UPR and leads to an up-regulation of parkin. A. Parkin mRNA levels are increased in response to mitochondrial membrane dissipation induced by CCCP. SH-SY5Y cells were incubated with 10 μM CCCP for the indicated time. Cells were harvested and total cellular RNA was isolated and subjected to quantitative RT-PCR using parkin-specific primers. The amount of RNA of each sample was normalized with respect to the endogenous housekeeping gene β-actin. Shown is the fold increase of parkin-specific mRNA compared with untreated control cells. **B.** Parkin mRNA is up-regulated upon CCCP treatment in primary mouse cortical neurons. Primary cortical neurons derived from embryonic mouse brain were incubated with CCCP (10 μM) for 12 h and analyzed as described in A. **C.** Human, mouse, bovine and equine promoter sequences of parkin, which are elongated downstream of the transcription start site (TSS) by 150 bp. Red arrow indicates the TSS and positions are denoted relative to the TSS. The CREB/ATF-binding sites are indicated by semicircles. Red, yellow and blue semicircles are predicted by three different binding motifs, which correspond to a Genomatix-defined family of 14 matrices describing the CREB/ATF-binding site. The red and yellow colored binding site is conserved between *Homo sapiens*, *Bos taurus* and *Equus caballus*, and *Homo sapiens* and *Equus caballus*, respectively, whereas the blue binding site is conserved across all four species. The green semicircles (not conserved) are additional binding sites. Downstream of the TSS, in the first intron of the parkin gene, an additional CREB/ATF-binding site is located in *Homo sapiens*, *Mus musculus* and *Bos taurus*. The consensus ATF4-binding site is written in bold letters. hsa, *Homo sapiens*; mmu, *Mus musculus*; bta, *Bos taurus*; eca, *Equus caballus*. **D, E.** CCCP activates the UPR and causes ER stress. **D.** The ER stress luciferase reporter construct ERSE-II-luc (**ER s**tress response **e**lement II) is activated by CCCP. HEK293T cells were transfected with the ERSE-II-luc reporter. 24 h after transfection, the cells were treated

with 10 μM CCCP for 24 h. As a positive control the cells were treated with the ER stressor tunicamycin (2 μg/ml, 24 h). Shown is the fold induction of luciferase activity in CCCP-treated cells in comparison to non-treated control cells. Quantification is based on triplicates of at least 3 independent experiments. **E.** BiP expression is increased in response to CCCP treatment. As an indicator of ER stress BiP mRNA levels were analyzed in SH-SY5Y cells treated with CCCP (10 μM) for the indicated time by quantitative RT-PCR as described in Fig. 1 A. Tunicamycin (2 μg/ml) was used as a positive control to induce ER stress. *** $p < 0.001$, ** $p < 0.01$.

Fig. 2. Parkin gene expression is up-regulated in response to ER stress. A, B. Parkin mRNA levels are increased under ER stress induced by thapsigargin or tunicamycin. SH-SY5Y cells were incubated with 1 μM thapsigargin (TG) (A) or 2 μg/ml tunicamycin (TM) (B) for the indicated time. Cells were harvested and total cellular RNA was isolated and subjected to quantitative RT-PCR using parkin-specific primers. The amount of RNA of each sample was normalized with respect to the endogenous housekeeping gene β-actin. The same results were obtained when 18sRNA was used as a control gene (data not shown). Shown is the fold increase of parkin-specific mRNA compared with untreated control cells. **C.** Amino acid starvation leads to the up-regulation of parkin mRNA. SH-SY5Y cells were treated with 2 mM L-histidinol in cell culture medium containing 10% dialysed FCS for 14 h. The cells were then harvested and total cellular RNA was isolated and subjected to quantitative RT-PCR using parkin-specific primers as described under Fig. 1 A. **D-F.** Parkin protein expression is increased after ER stress induced by TG, TM, or amino acid starvation. Expression of endogenous parkin after treatment of SH-SY5Y cells with TG (D), TM (E) or L-histidinol (F) for 14 h was analyzed by Western blotting using the anti-parkin mAb PRK8. Loading was controlled by re-probing the blots for β-actin. The Western blot image (E) was

re-arranged by excluding one line, as indicated by a white line; all samples originate from one gel. **G-I.** Parkin mRNA is up-regulated upon ER stress in HEK293T cells, mouse embryonic fibroblasts, and primary mouse cortical neurons. HEK293T cells (G), mouse embryonic fibroblasts (H), or primary cortical neurons derived from embryonic mouse brain (I) were incubated with TG (1 μM) or TM (2 μg/ml; primary cortical neurons: 3 μg/ml) for 12 h or 8 and 12 h (primary cortical neurons) and analyzed as described in A. *** $p < 0.001$, ** $p < 0.01$, * $p < 0.05$.

Fig. 3. Transcriptional up-regulation of parkin under ER stress is mediated by ATF4. A. Schematic representation of the consensus ATF4-binding site, the putative ATF4-binding site within the parkin promoter and the luciferase reporter constructs cloned for the analysis described in the following: park-luc contains the putative ATF4-binding site of the parkin promoter in triplicate, mutant park-luc habors two point mutations within the putative ATF4-binding site, and ATF4RE-luc contains the confirmed ATF4-binding site of the insulin growth factor binding protein 1 (IGFBP1) promoter in triplicate. Of note, the putative binding site for ATF4 within the parkin promoter is located on the complementary strand in 5'→3' direction. **B.** The park-luc reporter construct is induced after ER stress. HEK293T cells or SH-SY5Y cells were transfected with either the control luciferase reporter construct pGL3-luc (vector), the ATF4RE-luc construct containing the confirmed ATF4-binding site, the park-luc construct or the park-luc construct with a mutated ATF4 binding site (mut. park). 8 h after transfection cells were incubated with 1 μM thapsigargin (TG) and harvested after 14 h of treatment. Shown is the fold induction of luciferase activity in stressed cells compared to the non-stressed control based on triplicates of at least 3 independent experiments. **C.** Increased expression of ATF4 or upstream PERK induces transcription from the park-luc reporter construct. HEK293T cells were co-transfected with the ATF4RE-luc reporter plasmid or the park-luc reporter plasmid and ATF4, PERK, or GFP (as a control). As a positive control one

set of cells was treated with TG as described under B. Shown is the fold induction of luciferase activity compared to GFP-expressing control cells based on triplicates of at least 3 independent experiments (left panel). Expression levels of ATF4 and PERK were analyzed by immunoblotting using the anti-ATF4 pAb C-20 or the anti-myc mAb 9E10 (right panels). Notably, TG treatment (1 μM, 14 h) induced the increased expression of endogenous ATF4. Loading was controlled by re-probing the blots for β-actin. **D.** A dominant negative mutant of ATF4 (ATF4ΔN) interferes with the activation of the park-luc reporter construct in response to ER stress. HEK293T cells were co-transfected with the park-luc reporter plasmid and ATF4, ATF4ΔN, or GFP (as a control). 8 h after transfection cells were incubated with 1 μM TG for 14 h. Shown is the fold induction of luciferase activity in comparison to GFP-expressing control cells based on triplicates of at least 3 independent experiments (left panel). Expression levels of ATF4 and ATF4ΔN were analyzed by immunoblotting using the anti-ATF4 pAb C-20 (right panel). Loading was controlled by re-probing the blots for β-actin. *** $p < 0.001$, ** $p < 0.01$, n.s. = not significant.

Fig. 4. ATF4 binds to the parkin promoter and mediates parkin up-regulation in response to ER and mitochondrial stress. A. ER and mitochondrial stress-induced up-regulation of parkin is impaired in ATF4-deficient cells. SH-SY5Y cells were transfected with ATF4-specific or control siRNA duplexes. 2 days later cells were re-transfected with siRNA duplexes and then incubated with 1 μM TG or 10 μM CCCP for 14 h. The cells were harvested and analyzed as described in Fig. 1 A by quantitative RT-PCR using parkin-specific or ATF4-specific primers. The amount of RNA of each sample was normalized with respect to β-actin. Shown is the fold increase of parkin mRNA in response to TG or CCCP treatment left panel). The efficiency of ATF4 downregulation was determined by quantitative RT-PCR (right panel) and Western blotting (lower right panel) using the anti-ATF4 pAb C-20. **B.** ER

stress-induced up-regulation of parkin is impaired in primary cortical neurons from ATF4 knockout mice. Primary cortical neurons from ATF4-deficient or wildtype mice were treated with tunicamycin (3 μg/ml) for 8 h. Total RNA was isolated and analyzed using parkin-specific primers as described in Fig. 1 A. **C.** ATF4 binds to the parkin promoter *in vivo*. HEK293T cells or SH-SY5Y cells incubated with or without 300 nM TG for 2 and 8 h were used to perform a ChIP analysis using a pAb specific for ATF4 in comparison to a non-specific rabbit IgG. For the final real time PCR step, primers specific for the parkin promoter region were used. *** $p < 0.001$, ** $p < 0.01$, * $p < 0.05$.

Fig. 5. c-Jun suppresses the up-regulation of parkin after ER stress. A. c-Jun binds to the parkin oligonucleotide harboring the CREB/ATF-binding site. HEK293T cells were incubated with 2 μM thapsigargin (TG) and harvested after 3 h. Nuclear extracts were prepared and tested for binding to the ^{32}P-labeled oligonucleotide comprising the putative ATF4-binding site within the parkin promoter (park oligo; lanes 1-5) by an electrophoretic mobility shift assay (EMSA). The labeled oligonucleotides were incubated with nuclear extracts in the absence or presence of a 100-fold excess of unlabeled park oligo (lane 5) to compete with the binding reaction. To test for supershift activity, the anti-c-Jun pAb (N) sc-45X (lane 3) or the anti-ATF4 pAb C-20 (lane 4) was added to the binding reaction. **B.** c-Jun decreases transcription from the park-luc reporter after ER stress. HEK293T cells were co-transfected with the park-luc reporter construct and c-Jun or GFP (as a control). 8 h after transfection, the cells were treated with 1 μM TG for 14 h. Shown is the fold induction of luciferase activity in c-Jun-expressing cells in comparison to GFP-expressing control cells based on triplicates of at least 3 independent experiments. Expression levels of c-Jun were analyzed by immunoblotting using the anti-c-Jun pAb (N) sc-45 (lower panel). 3 μg protein of total cell lysates were loaded. Loading was controlled by re-probing the blots for β-actin. **C.** c-Jun suppresses the ATF4-mediated activation of the park-luc construct. HEK293T cells were co-

transfected with the park-luc reporter plasmid and either GFP (as a control), ATF4 plus GFP or ATF4 plus c-Jun. 8 h after transfection, the cells were treated with 1 μM TG for 14 h. Shown is the fold induction of luciferase activity in ATF4-expressing cells in comparison to ATF4- and c-Jun-expressing cells based on triplicates of at least 3 independent experiments. Expression levels of ATF4 and c-Jun were analyzed by immunoblotting using the anti-ATF4 pAb C-20 or the anti-c-Jun pAb (N) sc-45. 3 μg protein of total cell lysates were loaded. Loading was controlled by re-probing the blots for β-actin (lower panel). **D.** ER stress induced up-regulation of parkin is increased in c-Jun-deficient cells. SH-SY5Y cells were transfected with c-Jun-specific or control siRNA duplexes. 1 day later cells were re-transfected with siRNA duplexes and incubated with 1 μM TG for 14 h. The cells were harvested and analyzed as described in Fig. 1 A by quantitative RT-PCR using parkin-specific primers. The amount of RNA of each sample was normalized with respect to β-actin. Shown is the fold increase of parkin mRNA in response to TG treatment (upper panel). The efficiency of c-Jun downregulation was determined by Western blotting using the anti-c-Jun anti-c-Jun pAb (N) sc-45 (lower panel). 30 μg protein of total cell lysates were loaded. **E.** JNK3 decreases transcription from the park-luc reporter. HEK293T cells were co-transfected with the park-luc reporter plasmid and JNK3 or GFP (as a control). 24 h after transfection, the cells were treated with 1 μM TG for 8 h. Shown is the fold induction of luciferase activity in JNK3-expressing cells in comparison to GFP-expressing control cells based on triplicates of at least 3 independent experiments. Expression levels of JNK3 were analyzed by immunoblotting using an anti-JNK pAB (lower panel). Loading was controlled by re-probing the blots for β-actin. **F.** The JNK inhibitor SP600125 increases parkin up-regulation in response to ER stress. SH-SY5Y cells were treated with or without the JNK inhibitor SP600125 (10 μM) for 24 h. Thapsigargin was added after 10 h for additional 14 h. To quantify parkin-specific mRNA, cells were harvested and analyzed as described in Fig. 1 A

for quantitative RT-PCR using parkin-specific primers. The amount of RNA of each sample was normalized with respect to β-actin. Shown is the fold increase of parkin mRNA. Parkin protein levels were analyzed by immunoblotting using an anti-parkin PRK8 mAb (lower panel). The efficiency of SP600125 was controlled by blotting against phosphorylated c-Jun using the phospho-specific anti-c-Jun antibody X (Ser63) II pAb. 15 μg protein of total cell lysates were loaded. Loading was controlled by re-probing the blots for c-Jun and β-actin. *** $p < 0.001$, ** $p < 0.01$, * $p < 0.05$.

Fig. 6. Parkin protects cells from ER stress-induced cell death. A. Increased expression of wildtype parkin protects cells from ER stress-induced cell death. SH-SY5Y cells were co-transfected with EYFP (as a control) and wildtype parkin or the pathogenic parkin mutants G430D or ΔUBL. 24 h after transfection, cells were incubated with 10 μM thapsigargin (TG) or 5 μg/ml tunicamycin (TM) at 37°C for 8 h, fixed, permeabilized, and then the activation of caspase-3 was analyzed by indirect immunofluorescence using an anti-active caspase-3 pAb. Shown is the percentage of apoptotic cells among transfected cells. Parkin expression levels were determined by immunoblotting using the anti-parkin PRK8 mAb. Loading was controlled by re-probing the blots for β-actin (lower panel). **B.** Parkin-deficient cells are more vulnerable to ER stress-induced cell death. SH-SY5Y cells were transfected with parkin-specific or control siRNA duplexes and co-transfected with EYFP (as a control) or siRNA-resistant wildtype parkin (rescue parkin). 3 days later the cells were stressed with TG (10 μM) for 8 h fixed, permeabilized, and then the activation of caspase-3 was analyzed by indirect immunofluorescence as described in A. Parkin expression levels were determined by immunoblotting using the anti-parkin PRK8 mAb. Loading was controlled by re-probing the blots for β-actin (lower panel). **C.** Mouse embryonic fibroblasts (MEFs) derived from parkin knockout mice are more vulnerable to ER stress than wildtype MEFs. MEFs from wildtype

(WT) or parkin knockout (KO) mice were stressed with TG (10 μM) for 16 h and then cellular viability was determined by the MTT assay. Shown is the relative viability of KO MEFs in comparison to WT MEFs after TG treatment. Quantification is based on five independent experiments. **D.** Skin fibroblasts of patients carrying pathogenic mutations in the parkin gene are more vulnerable to ER stress. Skin fibroblasts from patients and control indivduals were stressed with tunicamycin (TM, 10 μM) for 24 h, fixed, permeabilized, and then the activation of caspase-3 was analyzed by indirect immunofluorescence as described in A. *** $p < 0.001$, ** $p < 0.01$, * $p < 0.05$.

Fig. 7. Parkin has no direct effect on ER stress. A. Parkin deficiency does not increase the level of ER stress. SH-SY5Y cells were transfected with parkin-specific or control siRNA duplexes. 3 days later the cells were stressed with 1 μM thapsigargin (TG) for 5 h. As an indicator of ER stress BiP mRNA levels were analyzed by quantitative RT-PCR as described in Fig. 1A (left panel). To test for the efficiency of parkin knockdown, parkin mRNA levels were quantified in parallel (right panel). **B.** The level of ER stress is not increased in mouse embryonic fibroblasts (MEFs) derived from parkin knockout mice. MEFs from wildtype (WT) or parkin knockout (KO) mice were stressed with 1 μM TG or 2 μg/ml tunicamycin (TM) for 5 h. The levels of BiP mRNA were analyzed by RT-PCR as described in Fig. 1 A. **C.** Overexpression of parkin has no influence on the ER stress level determined by ER stress reporter constructs. HEK293T cells were co-transfected with the ER stress reporter plasmids indicated (Supplemental Fig. 5) and either parkin or GFP (as a control). 24 h after transfection, the cells were treated with 1 μM TG for 8 h. Shown is the fold induction of luciferase activity in parkin-expressing cells in comparison to GFP-expressing control cells. Quantification is based on triplicates of at least 3 independent experiments. Expression levels of parkin were analyzed by immunoblotting using the anti-parkin pAB 2132 (lower panel). Loading was controlled by re-probing the blots for β-actin. **D, E.** The protective activity of

parkin after ER stress is independent of the proteasome. **D.** The efficiency of proteasomal inhibition by epoxomycin was demonstrated by an accumulation of endogenous p53 and ubiquitylated proteins. For immunoblotting an anti-p53 and anti-ubiquitin mAb was used. Loading was controlled by re-probing the blots for β-actin. **E.** Proteasomal inhibition does not impair the protective activity of parkin. SH-SY5Y cells were cotransfected with EYFP (as a control) or wildtype parkin. 24 h after transfection, cells were incubated with 10 μM thapsigargin (TG) and/or epoxomycin (epox, 0.1 or 10 μM) for 8 h, fixed, permeabilized, and then activation of caspase-3 was analyzed as described in Fig. 6 A. *** $p < 0.001$, ** $p < 0.01$, n.s. = not significant.

Fig. 8. Parkin prevents mitochondrial damage and dysfunction induced by ER stress. A, B. Increased parkin expression suppresses ER stress-induced mitochondrial fragmentation. SH-SY5Y cells were transfected with parkin or mCherry (as a control). 1 day after transfection, the cells were treated with thapsigargin (TG, 1 μM for 5 or 16 h) or tunicamycin (TM, 2 μg/ml for 5 or 16 h). Mitochondria were visualized by life cell microscopy after incubating cells with the fluorescent dye DiOC6(3). **A.** The mitochondrial morphology was classified as tubular or fragmented (small rod-like or spherical mitochondria). Shown is the percentage of cells with fragmented mitochondria. Quantifications were based on triplicates of 3 independent experiments. Per experiment ≥ 300 cells per coverslip of triplicate samples were assessed. Expression levels of parkin were analyzed by immunoblotting using the anti-parkin pAb 2132 (lower panel). Loading was controlled by re-probing the blots for β-actin. **B.** Examples of mitochondrial morphologies of the experiment described in A. Treatment of cells with TG or TM causes a disruption of the tubular mitochondrial network, which can be suppressed by increased parkin expression. **C.** Parkin deficiency increases ATP depletion in response to ER stress. SH-SY5Y cells were transfected with parkin or control siRNA

duplexes. On day 2 after transfection, the cells were shifted to low glucose medium containing 3 mM glucose instead of 25 mM. On day 3 the cells were treated with 2 μg/ml tunicamycin (TM) for 5 h and the steady state cellular ATP levels were measured by a bioluminescence assay. Cultured cells derived from tumors derive almost all of their energy from aerobic glycolysis rather than mitochondrial oxidative phosphorylation, in addition, stimulation of glycolysis in the presence of glucose inhibits mitochondrial respiration. Therefore, low glucose concentrations in the medium forces the cells to relay on oxidative phosphorylation to generate sufficient ATP. *** $p < 0.001$, ** $p < 0.01$.

Fig. 9. Interplay between ER stress, mitochondrial stress and parkin. ER stress can induce mitochondrial damage, such as alterations in mitochondrial morphology and bioenergetics. *Vice versa*, mitochondrial stress can induce ER stress, reflected by the induction of the unfolded protein response (UPR). Parkin is transcriptionally up-regulated in response to both mitochondrial and ER stress via ATF4, a transcription factor of the UPR. The stress-induced transcriptional up-regulation of parkin is antagonized by c-Jun which is activated by the JNK pathway. Increased expression of parkin under stress conditions protects cells from stress-induced cell death, explaining the high vulnerability of parkin-deficient cells to cellular stress.

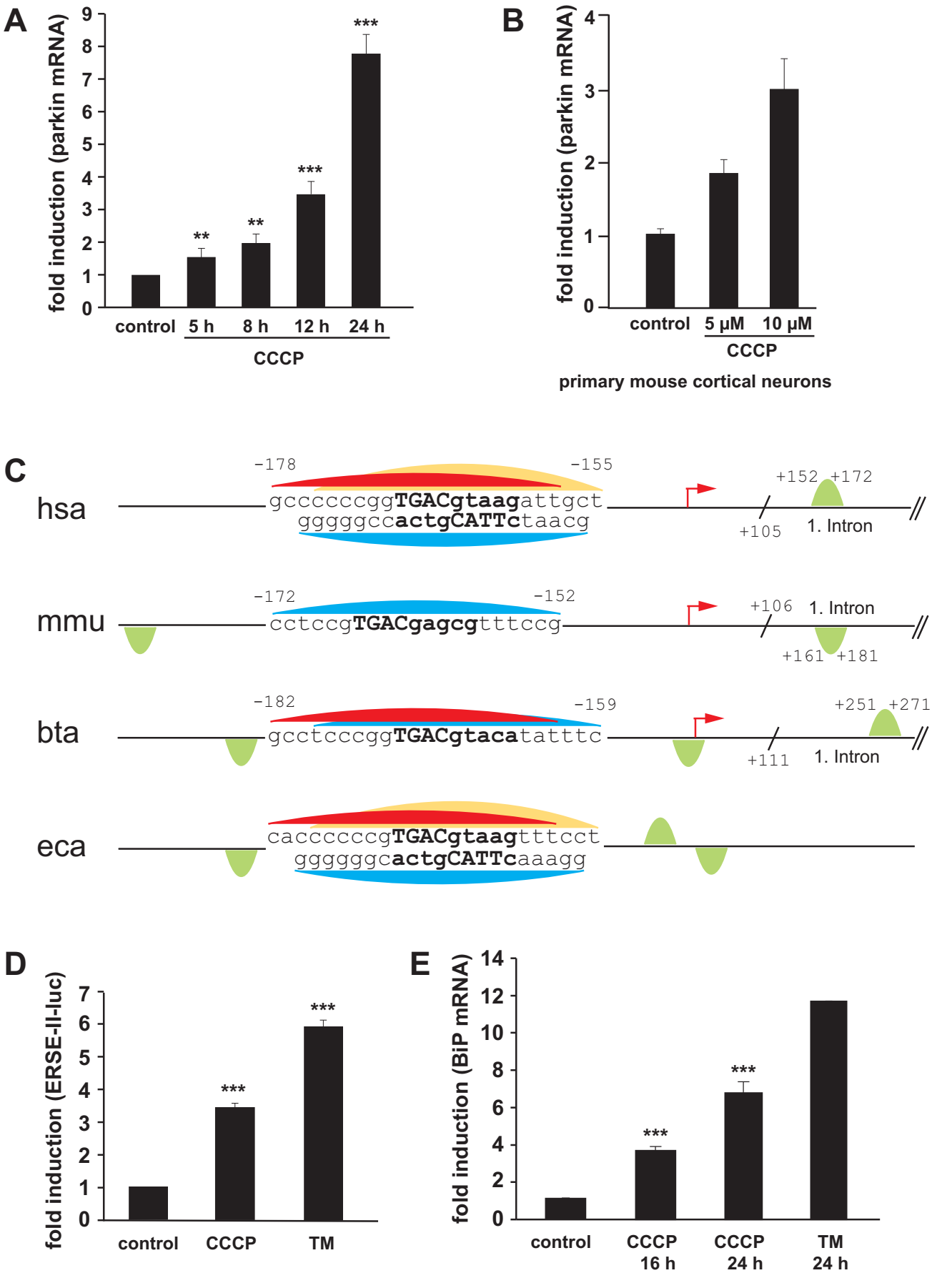
A
fold induction (parkin mRNA)
control
5 h
8 h
12 h
24 h
CCCP
B
fold induction (parkin mRNA)
control
5 µM
10 µM
CCCP
primary mouse cortical neurons
C
hsa
gccccccggTGACgtaagattgct
gggggccactgCATTctaacg
-178
-155
+152
+172
+105
1. Intron
mmu
cctccgTGACgagcgtttccg
-172
-152
+106
1. Intron
+161
+181
bta
gcctcccggTGACgtacatatttc
-182
-159
+251
+271
+111
1. Intron
eca
caccccccgTGACgtaagtttcct
gggggggcactgCATTcaaagg
D
fold induction (ERSE-II-luc)
control
CCCP
TM
E
fold induction (BiP mRNA)
control
CCCP 16 h
CCCP 24 h
TM 24 h

Figure 2, Bouman et al.

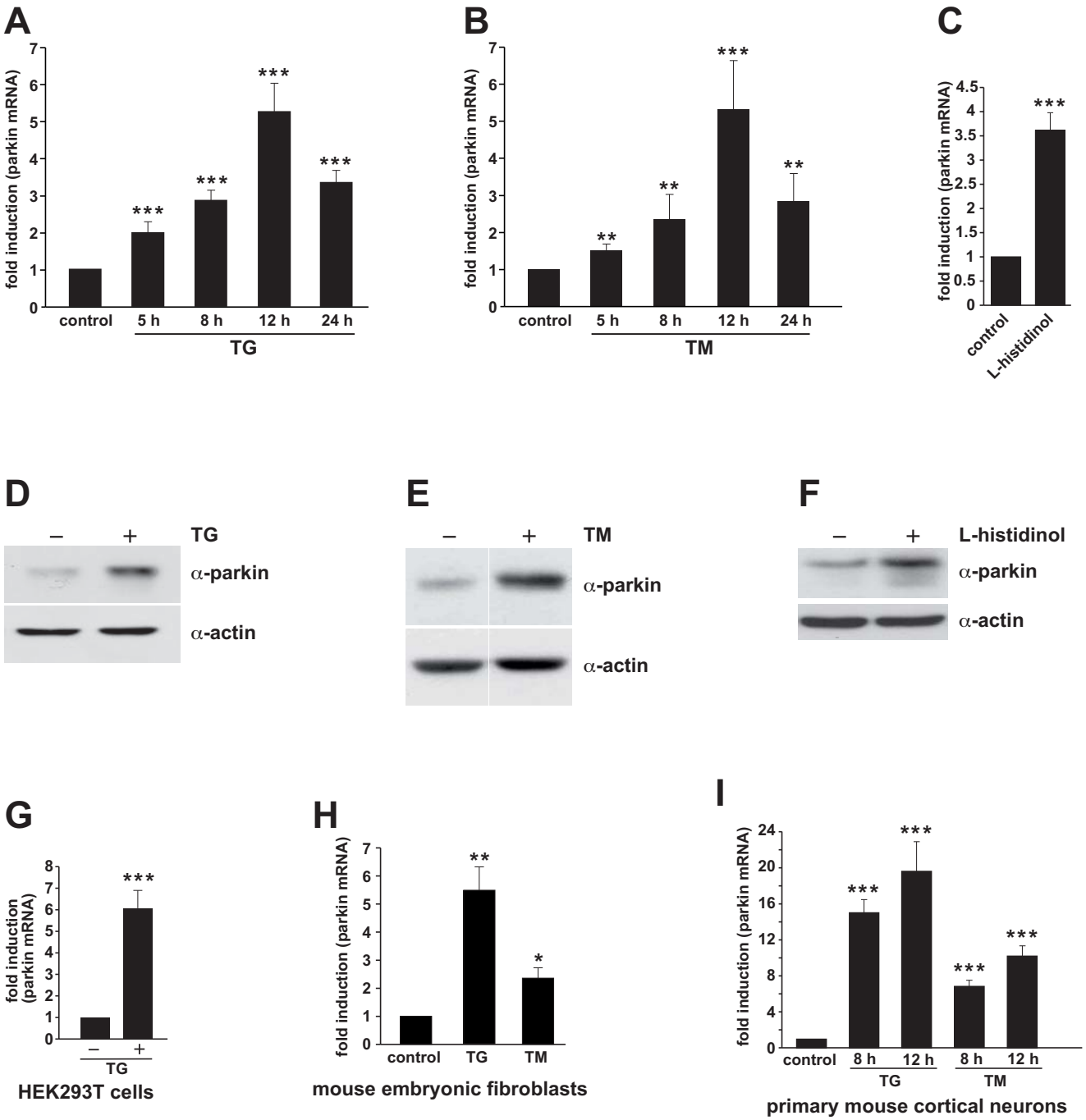

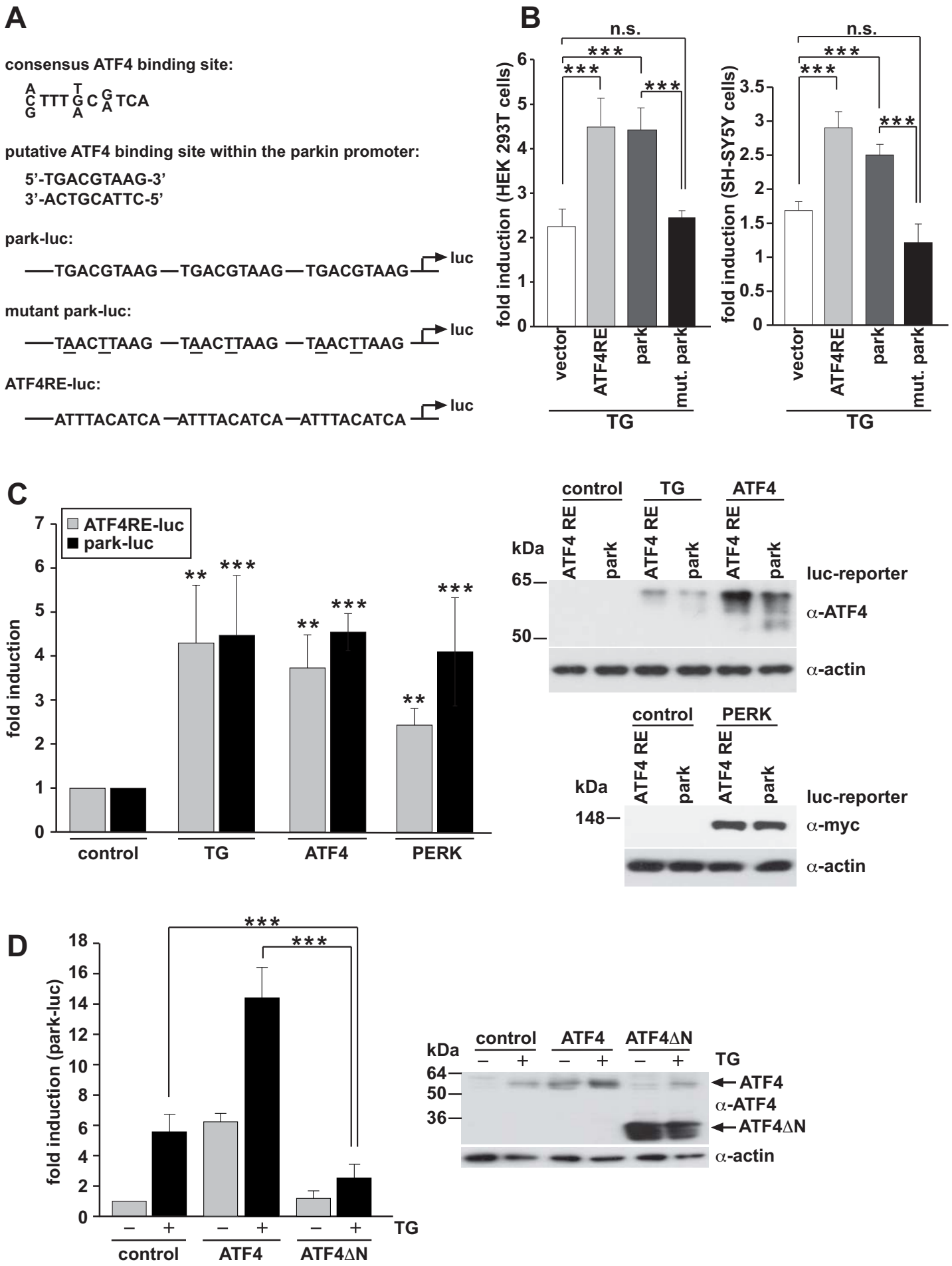
A
consensus ATF4 binding site:
A/C/G TTT T/G/A C G/A TCA
putative ATF4 binding site within the parkin promoter:
5'-TGACGTAAG-3'
3'-ACTGCATTC-5'
park-luc:
TGACGTAAG TGACGTAAG TGACGTAAG luc
mutant park-luc:
TAACTTAAG TAACTTAAG TAACTTAAG luc
ATF4RE-luc:
ATTTACATCA ATTTACATCA ATTTACATCA luc
B
n.s.
***
***
***
fold induction (HEK 293T cells)
fold induction (SH-SY5Y cells)
vector
ATF4RE
park
mut. park
TG
C
ATF4RE-luc
park-luc
fold induction
control
TG
ATF4
PERK
kDa
ATF4 RE
park
luc-reporter
65
50
α-ATF4
α-actin
148
α-myc
D
fold induction (park-luc)
TG
ATF4ΔN
64
36
ATF4
ATF4ΔN

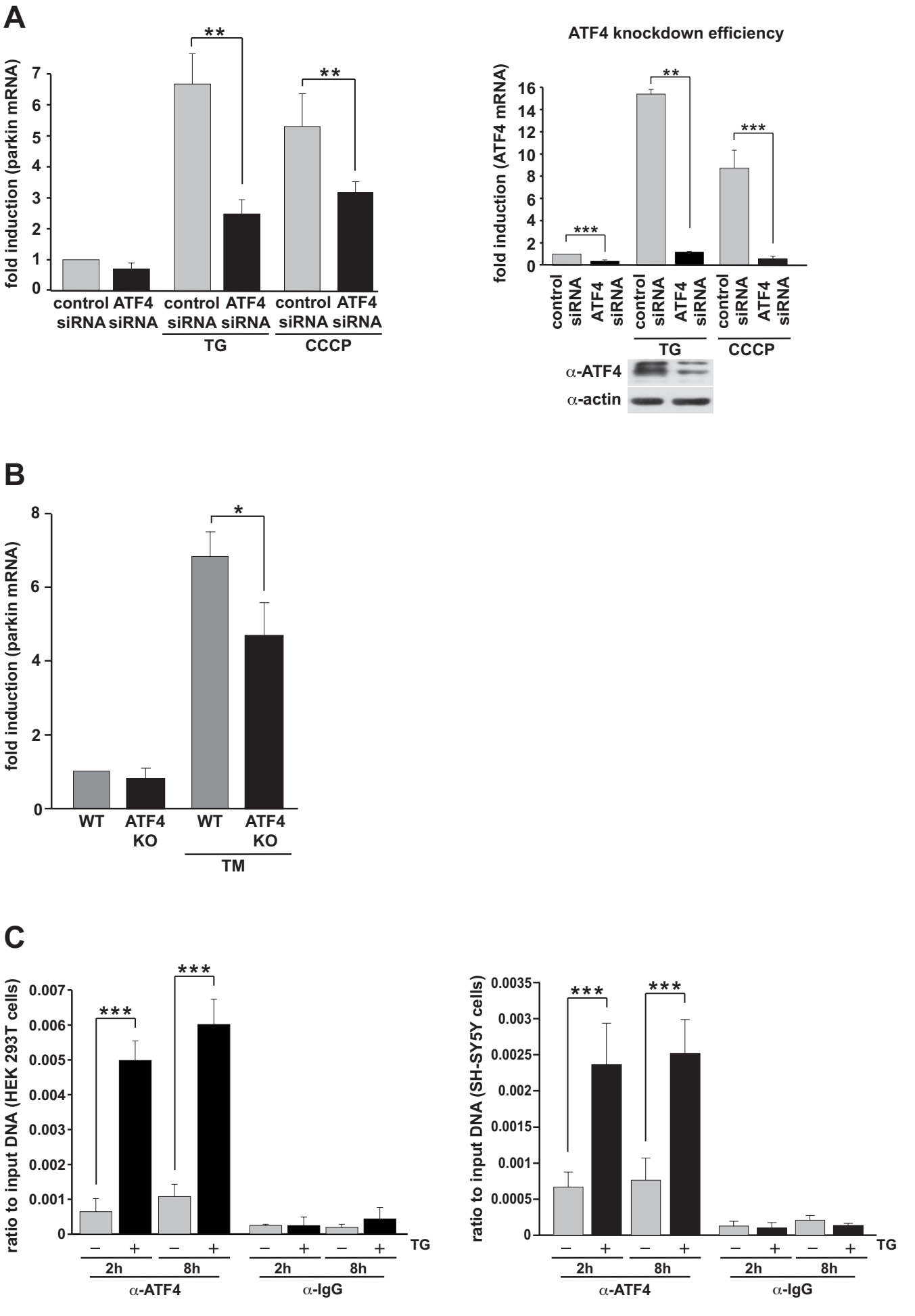
A
fold induction (parkin mRNA)
control siRNA
ATF4 siRNA
TG
CCCP
ATF4 knockdown efficiency
fold induction (ATF4 mRNA)
α-ATF4
α-actin
B
fold induction (parkin mRNA)
WT
ATF4 KO
TM
C
ratio to input DNA (HEK 293T cells)
ratio to input DNA (SH-SY5Y cells)
2h
8h
α-ATF4
α-IgG

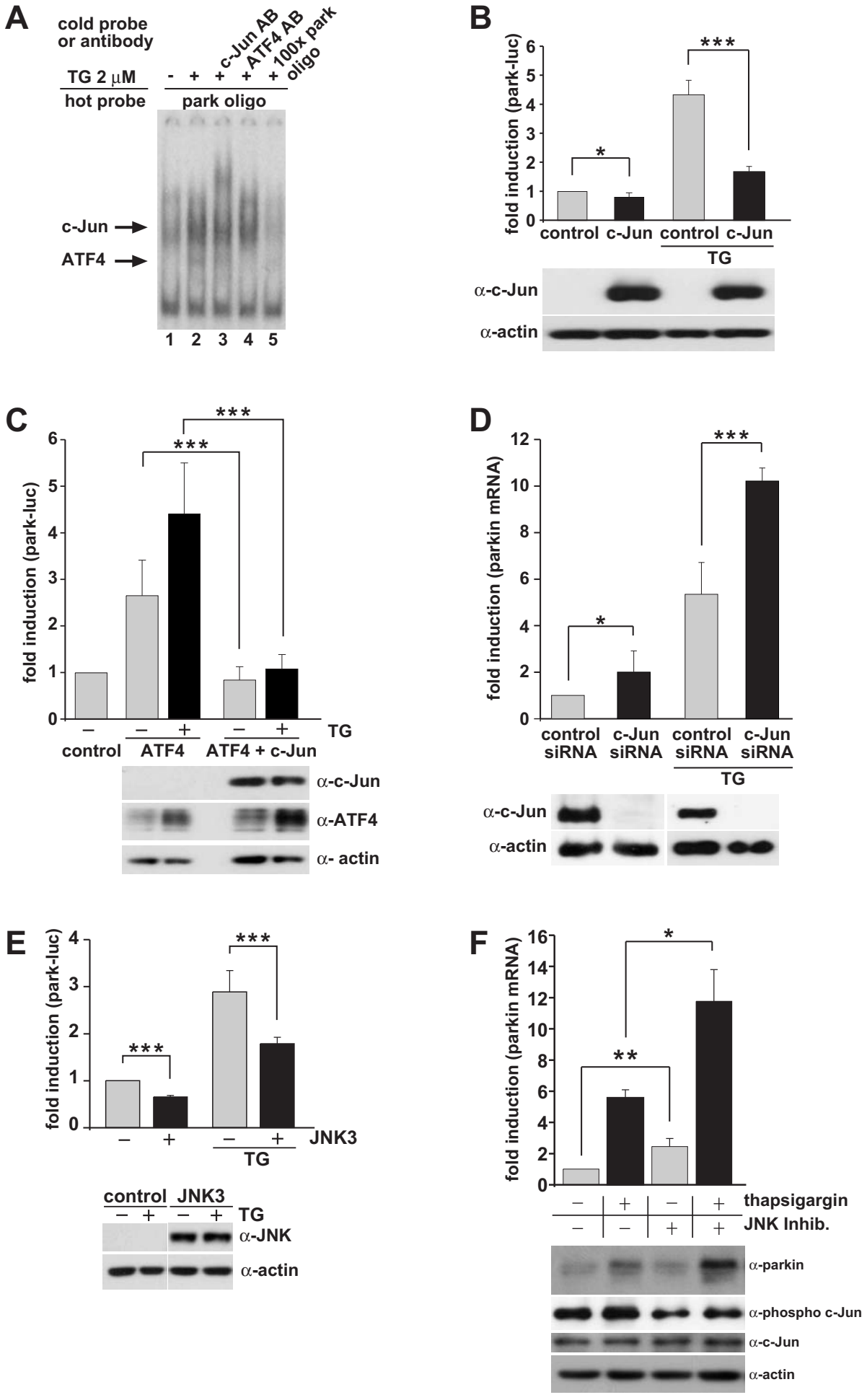
A
cold probe or antibody
c-Jun AB
ATF4 AB
100x park oligo
TG 2 μM
- + + + +
hot probe
park oligo
c-Jun
ATF4
1 2 3 4 5
B
fold induction (park-luc)
control c-Jun control c-Jun
TG
α-c-Jun
α-actin
C
fold induction (park-luc)
control ATF4 ATF4 + c-Jun
TG
α-c-Jun
α-ATF4
α- actin
D
fold induction (parkin mRNA)
control siRNA c-Jun siRNA control siRNA c-Jun siRNA
TG
α-c-Jun
α-actin
E
fold induction (park-luc)
JNK3
TG
control JNK3
TG
α-JNK
α-actin
F
fold induction (parkin mRNA)
thapsigargin
JNK Inhib.
α-parkin
α-phospho c-Jun
α-c-Jun
α-actin

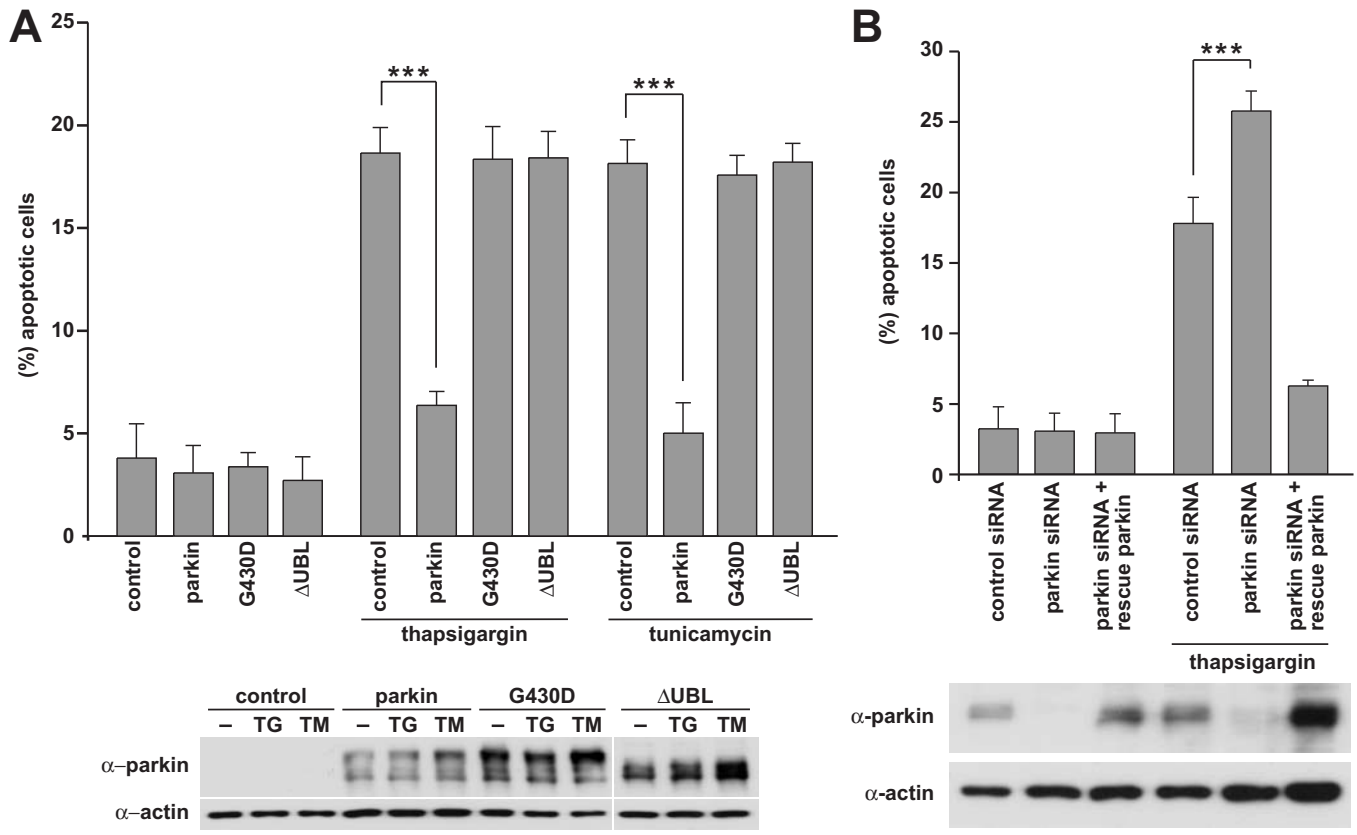
A
(%) apoptotic cells
control
parkin
G430D
ΔUBL
thapsigargin
tunicamycin
***
α–parkin
α–actin
B
(%) apoptotic cells
control siRNA
parkin siRNA
parkin siRNA + rescue parkin
thapsigargin
α-parkin
α-actin

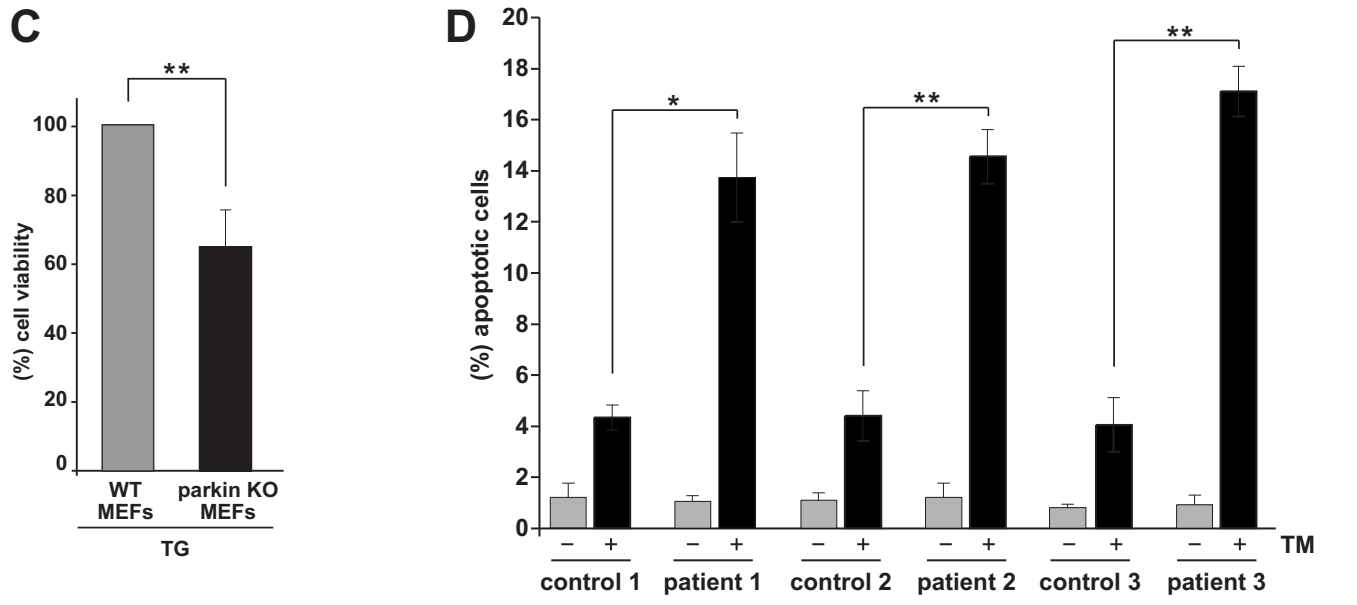
C
(%) cell viability
WT MEFs
parkin KO MEFs
TG
D
(%) apoptotic cells
control 1
patient 1
control 2
patient 2
control 3
patient 3
TM

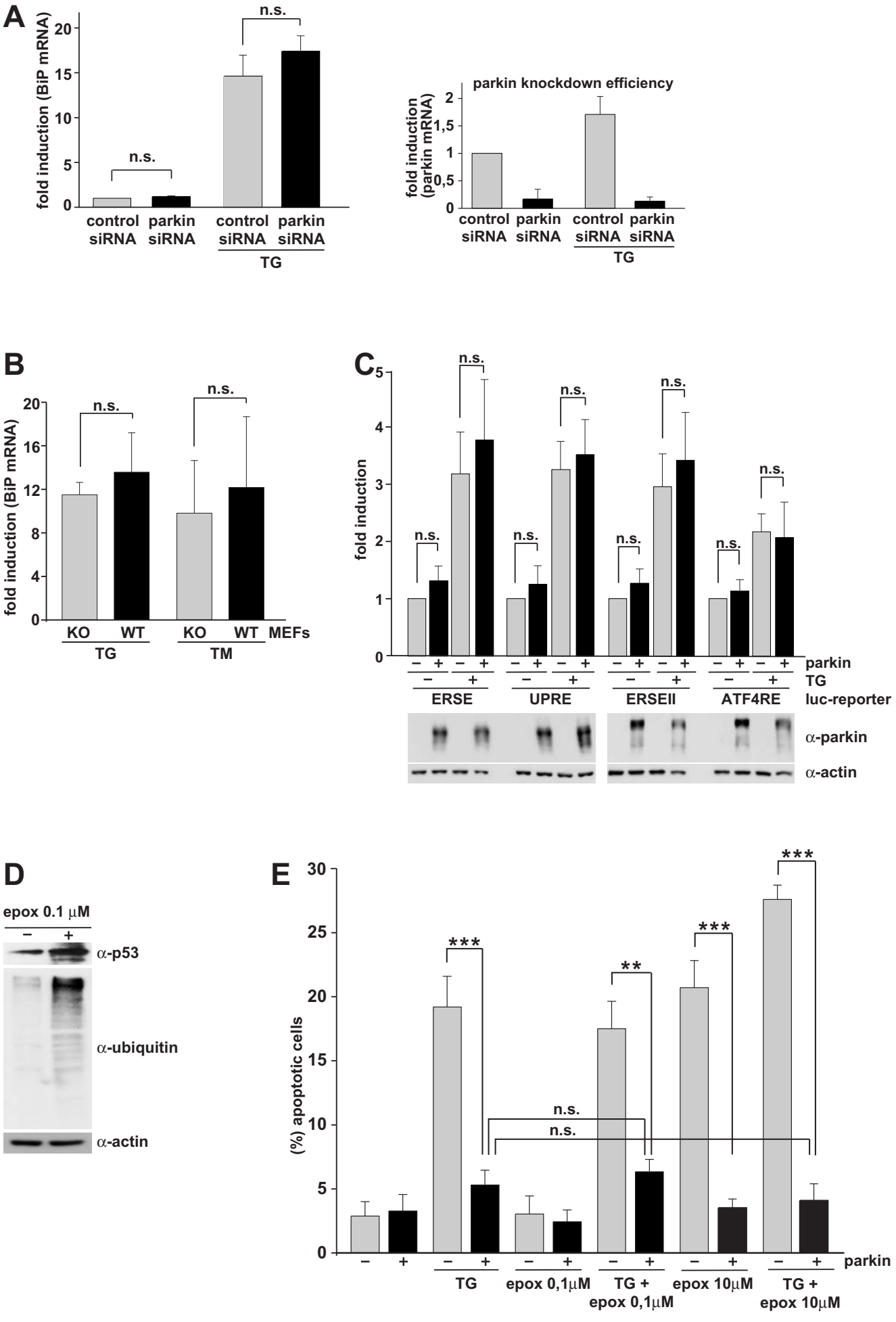
A
fold induction (BiP mRNA)
n.s.
n.s.
control siRNA
parkin siRNA
control siRNA
parkin siRNA
TG
parkin knockdown efficiency
fold induction (parkin mRNA)
B
fold induction (BiP mRNA)
KO
WT
KO
WT
MEFs
TG
TM
C
fold induction
parkin
TG
ERSE
UPRE
ERSEII
ATF4RE
luc-reporter
α-parkin
α-actin
D
epox 0.1 μM
α-p53
α-ubiquitin
α-actin
E
(%) apoptotic cells
***
**
n.s.
TG
epox 0,1μM
TG + epox 0,1μM
epox 10μM
TG + epox 10μM
parkin

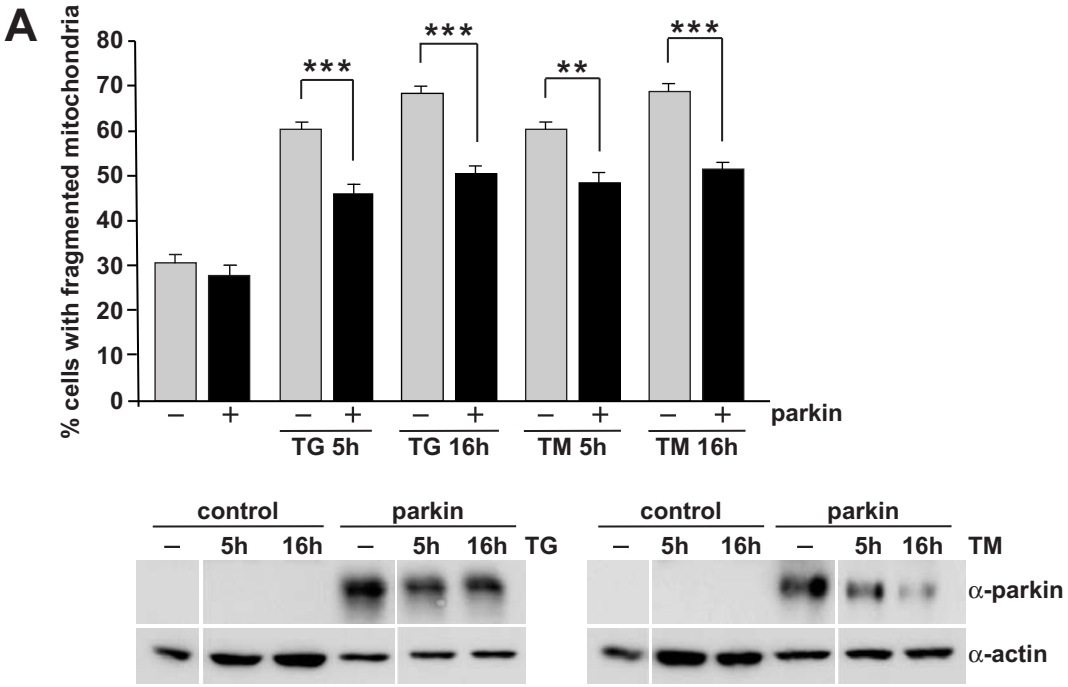
A
% cells with fragmented mitochondria
80
70
60
50
40
30
20
10
0
***
***
**
***
– + – + – + – + – +
parkin
TG 5h
TG 16h
TM 5h
TM 16h
control
parkin
– 5h 16h – 5h 16h TG
control
parkin
– 5h 16h – 5h 16h TM
α-parkin
α-actin

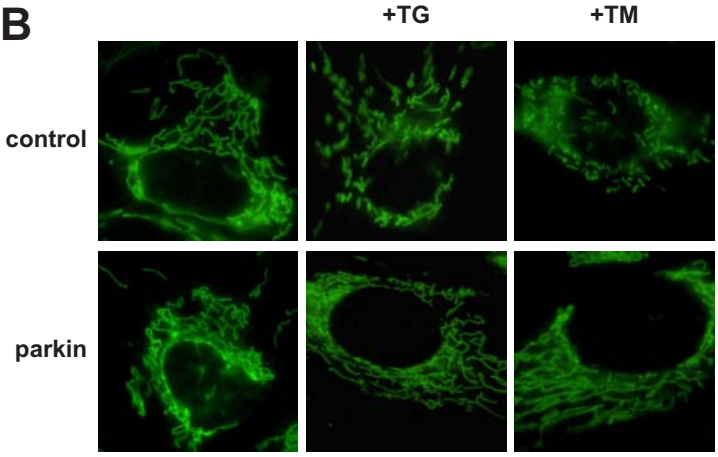
B
+TG
+TM
control
parkin

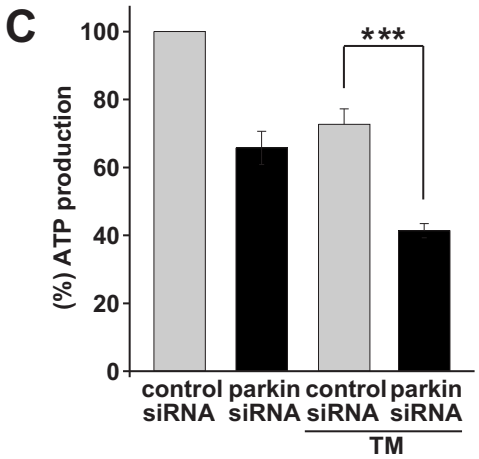
C
(%) ATP production
100
80
60
40
20
0
***
control siRNA
parkin siRNA
control siRNA
parkin siRNA
TM

Figure 9, Bouman et al.